Forestry Department
Food and Agriculture Organization of the United Nations

FRA 2000

THE ROLE OF REMOTE SENSING IN GLOBAL FOREST ASSESSMENT

A remote sensing background paper for Kotka IV expert consultation
01.07-05.07.2002, Kotka, Finland

Erkki Tomppo,

Raymond L. Czaplewski and Kai Mäkisara

Rome, 2002

Forest Resources Assessment Programme **Working Paper 61**
Rome 2002

The Forest Resources Assessment Programme

Forests are crucial for the well being of humanity. They provide foundations for life on earth through ecological functions, by regulating the climate and water resources and by serving as habitats for plants and animals. Forests also furnish a wide range of essential goods such as wood, food, fodder and medicines, in addition to opportunities for recreation, spiritual renewal and other services.

Today, forests are under pressure from increasing demands of land-based products and services, which frequently leads to the conversion or degradation of forests into unsustainable forms of land use. When forests are lost or severely degraded, their capacity to function as regulators of the environment is also lost, increasing flood and erosion hazards, reducing soil fertility and contributing to the loss of plant and animal life. As a result, the sustainable provision of goods and services from forests is jeopardized.

FAO, at the request of the member nations and the world community, regularly monitors the world's forests through the Forest Resources Assessment Programme. The Global Forest Resources Assessment 2000 (FRA 2000), reviewed the forest situation by the end of the millennium. FRA 2000 included country-level information based on existing forest inventory data, regional investigations of land-cover change processes and a number of global studies focusing on the interaction between people and forests. The FRA 2000 Main report published in print and on the World Wide Web in 2001.

The Forest Resources Assessment Programme is organized under the Forest Resources Division (FOR) at FAO headquarters in Rome. Contact persons are:

Peter Holmgren peter.holmgren@fao.org
Mohamed Saket mohamed.saket@fao.org

or use the e-mail address: fra@fao.org

Authors

Erkki Tomppo
Finnish Forest Research Institute, National Forest Inventory
Unioninkatu 40 A, FIN-00170 Helsinki, Finland
tel. +358 9 857 05 340, fax +358 9 625 308, e-mail: erkki.tomppo@metla.fi

Raymond L. Czaplewski
US Department of Agriculture, Forest Service
Rocky Mountain Research Station, Forest Inventory and Monitoring Environmetrics
2150 Centre Avenue Building A, Fort Collins, CO, 80526-1981 USA
tel. +1-970- 295 5973, fax, +1-970-295-5959, e-mail: rczaplewski@fs.fed.us

Kai Mäkisara
Finnish Forest Research Institute, National Forest Inventory
Unioninkatu 40 A, FIN-00170 Helsinki, Finland
tel. +358 9 857 05 334, fax +358 9 625 308, e-mail: kai.makisara@metla.fi

Table of Contents

Introduction, objectives and alternative remote sensing scenarios for FRA

The approach of FRA 2000 by FAO was the reliance on the participation of individual countries for both supply and analysis of information. It is hoped that this approach will lead for further capacity building in countries (FRA 2000 –main report). While countries firmly support this approach, it has sometimes been criticised on the basis that country information may be inaccurate, incomplete, out-of-date, or internationally inconsistent (Stokstad, 2001; Czaplewski, 2002). According to the FRA 2000 main report, many countries still lack reliable primary information at the national level. Some examples of country level changes in FRA 1990 and FRA 2000, as well as reliability assessment of TBFRA 2000, support this concern. One goal of the future assessments will be to further strengthen country capabilities and participation. In this way, FAO intends to improve the information quality as well as to assist developing countries in their inventories. FAO should also work towards reducing the interval between successive assessments, or towards the establishment of continuous regional assessments.

FAO conducted a remote sensing study of tropical forests in FRA 2000 for assessing the area changes between 1980-1990 and 1990-2000. Stratified sampling with a sampling ratio of 10 % was applied. The purpose was to independently evaluate the data quality of country information and to improve FAO's understanding of land-cover change processes in the tropics, especially deforestation, degradation, fragmentation and shifting cultivation, among others.

FAO also plans to continue to use country information and independent remote sensing surveys in future assessments, but also to emphasise field observations as a means of gathering broad and representative information.

For this purpose, the Forestry Department of FAO is developing a Global Forest Survey (GFS) (FAO, 2000). GFS have two main development objectives: 1: National Capacity building for sustainable forest management and 2) Forestry knowledge management for international processes. In addition to improving forest management and forestry knowledge management, the first objective is 'to support the member countries in establishing continuous forest resource assessment and monitoring systems and in developing their national capacities for the purpose', and 'to provide technical assistance to member countries in building national capacities in the areas of methodology development, use of new technologies and establishment of forest monitoring systems.' The second objective is 'to provide assessment variables required by international forestry processes, and establish feedback mechanism to evolve the collection of information and reporting over time', 'to develop a practical approach for the assessment and monitoring of the forestry resources at country and global levels that meets the concurrence of the member countries and donor community', and 'to establish, under the leadership of the FAO, partnership and co-operation linkages with well-established national and international institutions for the carrying out world wide forest survey in continuous basis'. According to the Working Paper (FAO, 2000), GFS 'should be regarded as a component of and development of FAO's global resource assessments, for which FAO has received a strong mandate from its member countries'.

The objective of this paper is to discuss opportunities to carry out a remote sensing aided forest resource survey (RSFS), independent of the countries' own inventories for the whole

globe. The emphasis is in the global level change estimates. For technical purposes, large region level estimates are also considered, e.g., estimates for Europe, North America, South America, with a possible differentiation into Temperate, Boreal and Tropical zones. The global level estimates are constructed from the large region level estimates.

The different opportunities for remote sensing data acquisition are presented. The properties of the sensors are presented in Appendix 2. Parameters that require quality control most urgently and for which the available resources give possibilities in RSFS are areas of forest land (FL), other wooded land (OWL) and other land (OL) as well as their changes. Tree stem volume and biomass are also key variables in assessing the status of worlds forests. The estimation of these variables requires thorough field measurements. The parameter estimation methods are discussed. We also demonstrate how the sampling designs and related errors could be evaluated from existing data sources, e.g., global land cover maps. This analysis is one of the main emphases of this paper and should be carried out with sufficient resources for a possible RSFS. The aim is neither to present real final sampling designs nor error estimates but rather outline methods which could be used in evaluating different designs when enough resources are available. Our study is presented in Appendix 1. The FRA 2000 global forest map of FAO (Zhu and Walter 2001) is applied in our study. Other land cover maps will probably be available when planning and realising a possible RSFS.

One of the basic questions in RSFS will be the availability of field data. Field sampling is needed because remote sensing based forest resource surveys should to be supported by field observations/measurements. Field sampling intensity depends on the available budget, variability of the target parameters in the field and the applied remote sensing material. Often, a minimum number of field plots is required for each image scene. A successful relative calibration of images may reduce this need.

Field measurements and designs are out of the focus of this paper. Possible rough cost estimates are presented if an independent sample will be collected. A possible field sampling design could be carried out utilising global land cover maps and same principles as presented in Appendix 1. Other possibilities for the field data include the GFS data or countries own data, provided by country correspondents and possibly evaluated by means of a sampling approach. GFS could also be used for a local evaluation of RSFS estimates.

The alternatives of RSFS vary depending on the ground sampling and remote sensing sampling densities. The variation can be illustrated in the space of 'Remote sensing intensity' and 'Field work intensity' dimensions (Figure 1). Both sampling densities are affected by the applied remote sensing material. The sampling intensities may vary also by regions, see Chapter 2.

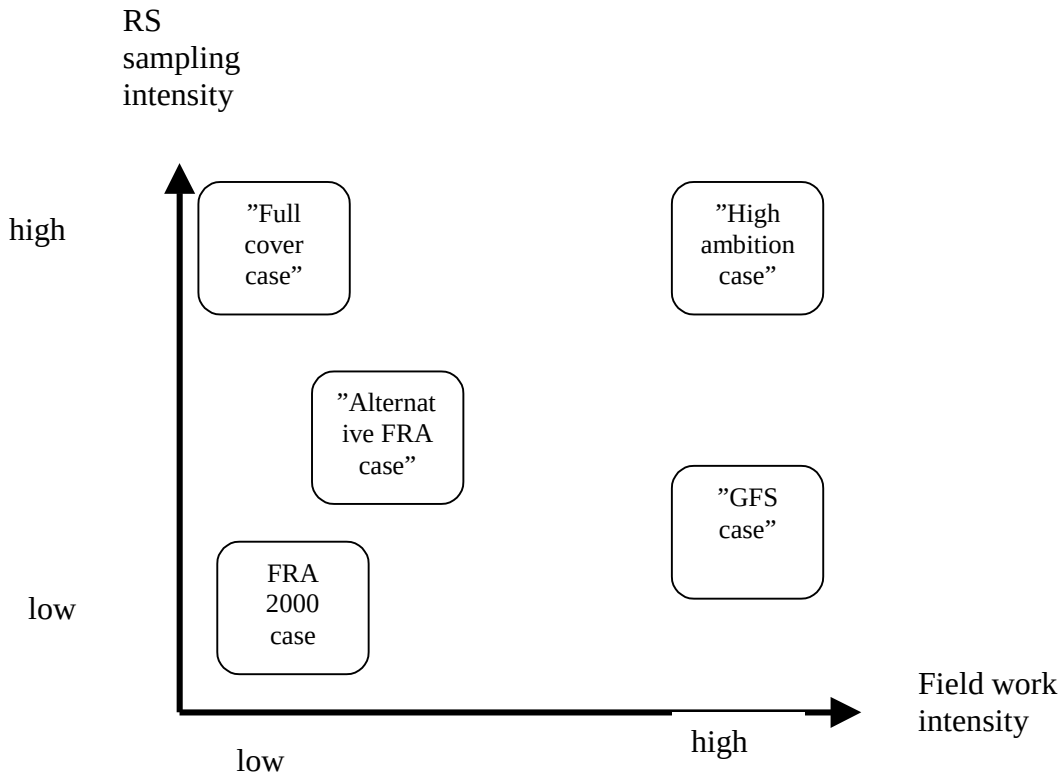

Figure 1: Examples of different sampling designs (adopted from Peter Holmgren)

1. Inventory regions and sub-regions

The regions of the independent remote sensing aided survey could be groups of countries, continents or sub-continents. For optimal sampling strategies, the regions can be further stratified into sub-regions on the basis of the vegetation zones, information needs, existing information and the possibilities of the control inventory, as well as remote sensing data (see, FAO 2001 b and Appendix 1). Regional designs are relevant because of specific information needs, technical reasons and variability of the target variables. Aggregation to global level is, however, the goal of the RSFS survey.

Analysis units can be determined on the basis of the variability of the variables of interest, e.g., percent forest or forest area change. The information from earlier assessments can be utilised in identifying the regions and analysis units. The land areas and forest areas of continents are given in Table 1(FAO 2001 a).

Table 1: Forest area by region 2000 (FAO 2001 a)

Region	Land area	Forest area	% of land area	% of all forests	Net change 1990-2000
	mill. ha	mill. ha			mill. ha/year
Africa	2978	650	22	17	-5.3
Asia	3085	548	18	14	-0.4
Europe	2260	1039	46	27	0.9
North and Central	2137	549	26	14	-0.6
America					
Oceania	849	198	23	5	-0.4
South America	1755	886	51	23	-3.7
Total	**13064**	**3869**	**30**	**100**	**-9.4**

Africa is divided into 6 sub-regions, Asia into 5, Europe into 4, North and Central America into 3, Oceania into 2 and South America into 2 sub-regions in FAO FRA 2000 main report (FAO 2001 a). These sub-regions, possible combined with vegetation zones, could be suitable sampling design units for RSFS. The optimisation with respect to changes may require more detailed stratification of the target areas. The changes are often clustered and local variation in changes is high (Drigo 2002). The highest relative change rates of the regions of Table 1 occur in Africa, South America and Oceania. A challenging task is to get a priori information about change hot spot areas. Remote sensing data, e.g., medium resolution data (Chapter 3), can be utilised in this task.

2. Review of methods

Two-stage stratified random sampling and visual interpretation of Landsat prints has been the approach in the global Tropical surveys in FRA 1990 and FRA 2000 (FAO 1996, FAO 2001 a, FAO 2001 b). The advantage of visual interpretation is the possibility to utilise contextual information and expert knowledge in the analysis more easily, sometimes in a more effective way, than in digital methods. Visual interpretation is especially effective for detecting changes in land use with images from different years. Visual interpretation is, however, laborious and is sensitive to subjective factors. These things become more critical in global surveys with varying vegetation zones. Visual interpretation may have some role, depending on the approach, e.g., in estimating reference data from very high resolution remote sensing data for digital analysis with high and medium resolution data, and also in feature extraction. Some most commonly used digital analysis methods are recalled in this chapter.

The traditional method applied in remote sensing has been discriminant analysis and its different versions. This method is relevant when the goal is to estimate a limited number classes, e.g., vegetation types or land cover classes (FL, OWL, other land). Regression analysis has been used estimating quantitative variables, e.g., tree stem volume and biomass. Non-parametric methods, e.g., k nearest neighbour estimation (k-nn estimation) and artificial neural networks have the advantages that they can be used for estimating simultaneously all inventory variables. Particularly, k-nn method is under intensive research in Europe and North America and has also been applied in operative inventories.

The availability of reference data for digital image analysis or visual image interpretation will be one key problem in remote sensing aided global survey. In principle, a certain minimum number of field plots for each image scene is needed. This could partly be overcome by relative calibration of images which makes it possible to utilise reference data from neighbouring image scenes.

Some details of the methods are summarised in the next sections.

2.1. Relative calibration of images

2.1.1. The physical model

Several mechanisms affect the electromagnetic signal carrying information from the targets on ground to the sensor above (on satellite or aircraft). The atmosphere attenuates the signal. The attenuation depends on the amount of air between the light source and the target, the amount of air between the target and the sensor, and the wavelength. The amount of air is dependent on the distance between the target and the sensor and this varies according to the location within the field of view of the instrument. Scattering of the light from the molecules of the different gases creates a background signal at each pixel in the image. This effect is also dependent on the wavelength and viewing geometry. In addition to this, the background level at a pixel is dependent on the neighbouring targets on ground. In total, any realistic

model of the atmospheric effects on the received signal is complex when the interaction between the electromagnetic field and the air is noticeable. In the microwave region the interaction is weak.

The reflection functions of natural targets vary according to the illumination and viewing angle. Models exist for predicting this phenomenon but, in addition to the viewing and illumination geometry, knowledge of the target is necessary and often not available beforehand.

Time is an important parameter in explaining the differences between images. If the images are from different dates, the atmospheric conditions are different. To some extent, the atmospheric conditions can be retrieved from the archived meteorological data or estimated from image data. The parameters related to the illumination and viewing geometry are easily available. The changes in the targets during time are more difficult to model.

Time is an important variable in explaining the changes within images if imaging takes a long time. This is the case in aerial image mosaics and airborne scanner data.

When analysing remote sensing images, all of the effects mentioned above must be somehow taken into account. In visual analysis, the human brain does this. If the analysis uses only a small region within a single image, the changes are small and can be ignored. When using global methods within larger images or images sets, correction must be applied or integrated into the analysis method.

The correction methods can be divided into two classes: atmospheric correction methods and relative calibration methods. The division is not exclusive. A correction system can include methods from both classes or relative calibration can be applied after atmospheric correction.

2.1.2. Atmospheric correction

The atmospheric correction methods correct single images based on a physical model and atmospheric parameters. The model is then inverted so that the target reflectance can be estimated for each pixel's ground footprint from the observed image pixel values.
The atmospheric models available (e.g., MODTRAN or 6S) (Berk et al. 1989, Vermote et al. 1997) are pretty good but the problem is availability of the atmospheric parameters. Good average values may be available but the parameters vary within an image covering a large area. In some cases it is possible to estimate this variability from the image data. Calibration of the sensors may also affect the results especially at low signal levels (e.g., in forested areas in the visible optical region). (It is very difficult to measure the changes in the sensor properties after the satellite has been launched).

Implementation of complete inversion of the atmospheric model at each pixel is not feasible but good enough approximations can be used with current computers. The atmospheric correction can be expected to compensate the atmospheric effects within images and between images to a large extent but absolute calibration of images is not feasible with current technology.

2.1.3. Relative calibration

The relative calibration methods try to make the images homogeneous and remove the differences between images. The physical mechanisms or other causes of the differences are not explicitly used, although methods may try to avoid removing changes related to the phenomena being examined (for instance, changes in forest between two time points).

The methods for relative calibration examine areas covered by two or more images or compute statistics for different parts of the images. These are then used to compute parameters for correction models.

The relative correction methods can be very efficient in removing visible changes between images. The methods are not dependent on any physical parameters that may not be available. The drawback is the possibility of correcting differences due to variability in the target state.

2.2. Methods for delineating analysis units

Sometimes the analysis of larger units than a single pixel may improve the accuracy of the image analysis based estimates. This is the case particularly with very high resolution images and with visual interpretation. The analysis unit can be, e.g., a patch with a minimum area to be classified as forest land or a homogeneous forest area. Segmentation methods are applied in digital image analysis in delineating the area of interest to subsets. Segmentation can be done either using multitemporal images, the difference image or a single image.

Image segmentation means partitioning the image into homogeneous areas according to some criterion. The homogeneity criterion is selected to either result in areas meaningful for the application area (for instance, forest stands) or meaningful as an aid in analysis. The criterion is computed using the pixels belonging to each area. Segmentation is useful only if the resolution of images is high enough so that the meaningful entities in the image are larger than one pixel.

The segmentation methods compute a more or less optimal allocation of pixels into areas based on the selected homogeneity criterion. The algorithms can be classified into three classes: splitting methods, merging methods, and split/merge methods. The splitting methods start by allocating all pixels to the single area. This area is then recursively split until each of the resulting areas is homogeneous enough according to the selected criterion. The drawback of splitting methods is that they tend to result in an excessive number of areas. The merging methods start from elementary areas (for instance, pixels) and combine the areas as long as the combined areas are homogeneous enough. The drawback of these methods is also that the resulting areas will be smaller than the optimal partitioning. The split/merge methods alternate between the two basic methods to arrive at the optimal partitioning.

The practical segmentation methods can use quite complex homogeneity criteria. The criteria can combine spatial features within an area with edge features at the border of the area.

The value of segmentation can be twofold. In all cases it enables use of several pixels for computation of more reliable information for an entity than pure pixel wise methods. In some

cases the segments can also be meaningful to the application. One example is automatic partitioning of the forest into stands.

2.3. Feature analysis

The purpose of feature analysis is to compute from the remotely sensed information a set of numbers that the analyser (human or machine) can most efficiently use. Feature analysis does not increase the available information but makes it accessible to the analyser and suppresses the information that is not interesting in the current analysis.

The feature analysis methods for remote sensing images can be separated into point wise methods and spatial methods. The point wise methods compute new values based on the measurements from the same pixel. Examples are spectral channel ratios and difference images. The spectral channel ratios suppress unknown, useless information present in both channels in the ratio. One example is the average illumination level. Difference between data from two time points can be used to emphasise changes between the images. More elaborate point wise features can be constructed either based on physical or heuristical criteria.

The spatial features are computed from several pixels in the neighbourhood of the pixel being analysed. These features provide information about the spatial characteristics or homogeneity of the image around the pixel being analysed. Examples of spatial features are texture measures and edge detectors. The texture measures characterise the local regular or random structure of the intensity variations. A simple texture measure is the standard deviation of the intensities of the pixels in a small neighbourhood. A large number of more complex texture measures have been proposed in the literature. The edge detectors measure the probability of the pixel being on the border between two areas and possibly also the direction of the border at that point. These detectors are based on differences between neighbouring pixels.

2.4. Estimation using combined field measurements and remote sensing

Some commonly applied estimation and classification methods are recalled. These methods are often employed when field measurements and remote sensing data are available. The availability of other ancillary data, e.g., digital map data, reduces the errors of the estimates. A non-parametric k-nearest neighbour method is described in more detailed way as an example how the estimation procedure could be done, also when other data as remote sensing data and field data are available.

2.4.1. Discriminant analysis

Discriminant analysis is a widely used method to classify a satellite image area into pre-defined classes when field observations are available. Let us suppose that *n* classes have been defined (e.g., forest land, other wooded land, other land, or broad-leaved forest, coniferous forest, etc.). The probabilities of an arbitrary pixel *p* belonging to group *k*, are computed using discriminant functions based on the generalised quadratic distances:

$$D_k^2(y_p) = (y_p - m_k)' S_k^{-1} (y_p - m_k) + \ln|S_k| - 2\ln(q_k), \quad (1)$$

where

y_p is the vector of intensity values at pixel p,

m_k is an estimate of the vector of the expected intensities in class k,

S_k is an estimate of the covariance matrix of the intensities in class k, and

q_k is the prior probability of class k.

The value of q_k can be a'priori probability of each class or the inverse of the number of classes.

The posterior probability of observation y_p belonging to the class k is, under the multivariate normal assumption, obtained from equation (2):

$$p(k \mid y_p) = \frac{e^{-0.5 D_k^2(y_p)}}{\sum_{u=1}^{n} e^{-0.5 D_u^2(y_p)}} \quad (2)$$

where n is the number of classes.

The class with the highest posterior probability can be attached to the pixel p. Discriminant analysis or its variants might be relevant methods in RSFS if the purpose is to estimate the areas of land cover classes. Cross-validation can utilised in pixel level error estimation. Discriminat analysis is not necessarily the optimal method when several variables should be estimated simultaneously. Problems are the high number of classes and the preservation of the co-variance structure of the variables.

2.4.2. k-nn estimation

K nearest neighbour estimation method is under an intensive research among forest inventory groups (Nilsson 1997, Franco-Lopez et al. 2001, McRoberts et al. 2002, Tokola et al. 1996, Tomppo 1990). Its favour is based on the fact that it resembles the normal forest inventory estimation in the sense that certain weights for each field plot are employed in the estimation. It thus produces simultaneously the estimates for all inventory variables and preserves covariances between variables. Let's first recall the k-nn estimation method. It uses a distance metric, $d_{pi,p}$, defined in the image feature space. It is computed from pixel p to be analysed to each pixel p_i, whose ground truth is known (to pixel with sample plot i). Data from the k plots, $i_1(p),\ldots,i_k(p)$, with the shortest distances are utilised in the analysis of pixel p. A maximum distance in the geographical space (usually 50 to 100 km in the horizontal direction) is set

from the pixel *p* to the sample plots applied in order to avoid utilising sample plots from very different vegetation zones. A maximum distance is also set in the vertical direction (in south and central Finland, e.g., usually 50 to 200 m) in order to take into account the vegetation variation caused by elevation variation, provided that a digital terrain model is available. The feasible set of nearest neighbours for a pixel *p* was $\{p_i \in F \mid d_{p,p_i}^{(x,y)} \le d_{\max}^{(x,y)}, d_{p,pi}^{z} \le d_{\max}^{z}\}$, where *F* is o possible stratum from which the neighbours are sought, $d_{p,p_i}^{(x,y)}$ is the geographical horizontal and d_{p,p_i}^{z} geographical vertical distance from pixel *p* to pixel p_i and $d_{\max}^{(x,y)}$ and $d_{\max}^{z}$ their maximum allowed values.

The maximum distance in the geographical space can be compensated with a new method presented by Tomppo and Halme (2002). Variables describing the large scale variation of forest variables are used as additional variables in computing the distance metric in that method.

The weight of the ground data vector of plot *i* to pixel *p* is then defined by

$$w_{i,p} = \frac{1}{d_{p_i,p}^2} \Bigg/ \sum_{j \in \{i_1(p),\ldots,i_k(p)\}} \frac{1}{d_{p_j,p}^2}, \quad \text{if } i \in \{i_1(p),\ldots,i_k(p)\} \qquad (3)$$

= 0, otherwise.

Volume and biomass estimates can be written in the form of a digital map

$$\hat{m}_p = \sum_{j \in \{i_1(p),\ldots,i_k(p)\}} w_{j,p}\, m_j, \qquad (4)$$

where

$\hat{m}_p$ = the multi-source estimate of the value of variable *M* at pixel *p*, and

m_j = the measured value of variable *M* at field plot *j*.

The land use classes outside forestry land are transferred directly from digital map file (see Tomppo, 1990, 1996).

The sums of weights, $w_{i,p}$ were calculated by computation units (municipalities) in the estimation process. The weight of plot *i* to computation unit *U* is then:

$$c_{i,u} = \sum_{p \in u} w_{i,p}. \qquad (5)$$

The inventory statistics by computation units can be obtained by means of digital boundary maps and the weight coefficients (4). If preliminary land cover maps are available, the area of water and non-forestry land cover classes can be taken by computation units from the digital maps produced by multiplying the number of pixels classified in the land cover class by the size of the pixel:

$$A_{c,u} = \#(p \mid p \in c, p \in u)a, \qquad (6)$$

where

c = land cover class,

u = computation unit, and

a = area of one pixel.

The estimates of the areas of the forestry land reference units, by computation units, can be obtained from the estimated plot weights employing the equation

$$A_{s,u} = a\sum_{i \in I_s} c_{i,u}, \qquad (7)$$

where

S = forestry land reference unit (e.g., forest type),

I_S = set of sample plots belonging to the reference unit, and

u = computation unit.

Reduced weight sums $c^r_{i,u}$ are obtained from the formula (12), if clouds or their shadows cover a part of the area of the computation unit u. The real weight sum for plot i is estimated by means of the formula

$$c_{i,u} = c^r_{i,u} \frac{A_{s,u}}{A^r_{s,u}}, \qquad (8)$$

where

$A_{s,u}$ = area of the forestry land of unit u, and

$A^r_{s,u}$ = area of the forestry land of unit u not covered by the cloud mask.

It is thus assumed that the forestry land covered by clouds per computation units is, on average, similar to the rest of the forestry land with respect to the forest variables. The proportion of non-forestry land covered by clouds is estimated as given above.

The mean volume (and biomass) estimates by computation units can be obtained with the formula

$$v = \frac{\sum_{i \in I_s} c_{i,u} v_{i,t}}{\sum_{i \in I_s} c_{i,u}}, \qquad (9)$$

where s is a computation strata (e.g., forest land),
I_S the set of the sample plots in the strata,
u a computation unit,

$c_{i,u}$ the weight of the sample plot *i* in the unit *u*, and
$v_{i,t}$ the volume (biomass) per hectares of the growing stock on the sample plot *i*.

The total volume and biomass estimates are obtained by replacing the denominator in the Formula (9) by 1.

Most applications of the k-nn method concern the cases where digital land use map has been available. Methods for correction to a possible bias caused by incomplete map data have been presented by (Katila et al 2000, Katila and Tomppo 2002).

If the digital land use maps are not available, the weights (8) can be used also for area estimation outside of forest land (or forest and other wooded land) when all land use classes are represented among the field plots. McRoberts et al. (2002) used satellite images and field measurements together with k-nn estimation for reducing the RMSE of forest areas estimates without employing ancillary digital map data. The use of Landsat TM data together with field data reduced the variances of forest area estimates with a factor as great as 5 compared to field data based estimates. One field plot, consisting of four sub-plots, represented an area of 12 300 ha and 15 800 ha in two study areas. This sampling intensity and study are a relevant references to a possible remote sensing aided global survey.

The pixel level error of the estimates with remote sensing based methods are often high, particularly when estimating volumes or other quantitative variables (Tokola et al 1996, Nilsson 1997, Poso et al. 1999). The error, however, decreases rapidly when the area in question increases (Nilsson 1997, Tomppo et al. 2002). These studies are based on a relative dense grid of field plots and the use of remote sensing data is target to compute estimates for smaller areas than what is possible using. In the RSFS, the possible field plot is much more sparse and pilot studies are needed for error estimation.

2.4.3. Artificial neural networks

The artificial neural networks (ANN) are a group of information processing methods that are based on or inspired by principles from the biological neural systems. The networks consist of simple computational units with memory that are connected together using links. The connection weights are adjusted using a learning algorithm until the network performs the desired task. This task is basically a mapping from the set of input signals (for instance, reflectance of a target in different wavelength channels) to an output (for instance, classification of the pixel).

There are several different families of ANNs. Examples of the best known ANN types are Multilayer Perceptrons (MLP), Self-Organising Maps (SOM), Radial Basis Function (RBF) networks, ART (Adaptive Resonance Theory) networks. They differ in the unit type, connection topology, and learning algorithm. Each of the networks have advantages and drawbacks and no one family is clearly superior to another. Selection of the best family depends on the application.

One of the strongest advantages of neural networks is that the user does not have to specify a functional dependency between the inputs and outputs beforehand: the network learns the dependency when a set of learning samples if presented to the network. This enables the network to automatically infer and utilise very complex relationships between the input

signals and desired outputs. This is also a drawback because the networks may learn the dependencies between the learning samples instead of the general dependencies. The methods use learning parameters to balance the generality versus specificity and also the speed of learning.

The ANNs are effective tools in classification and estimation and they can sometimes give better results than classical statistical methods. ANNs have been tested also in many remote sensing tasks.

2.4.4. Regression analysis

A commonly used approach in regression analysis is to predict the variables of interest as a function of image features. A possible model is thus

$$A = f(\eta) + \varepsilon$$

where A is the variable to be predicted, η the vector of image features,

f a function whose parameters should be estimated and

ε a $N(0,\sigma^2)$ -distributed error term.

In local linear regression, a weighted model is fitted to each point η. The weight of an observation depends on distance of image features such that observations with nearby image features get higher weight. Ride regression can be used to reduce the effect of multi-collinearity. Regression analysis is suitable for instance for modelling and predicting volumes and biomass but can be applied with forest percentage as well.

3. Remote sensing material

3.1. Background

The current and some coming remote sensing sensors and their specifications are described in Appendix 2. The image prices are given when they are available. The remote sensing data can be divided into different categories using many criteria. The most important criteria are listed below.

The wavelength range: In principle, the remote sensing data can be based on any physical mechanism transferring energy between the target on the ground and the sensor on the remote platform (satellite, airplane, helicopter, balloon, etc.). In practice, the choices are limited by sensor technology, target properties, source of energy, the atmosphere between the target and the sensor, and the interaction of the target and the transfer mechanism. The only feasible alternative is electromagnetic radiation of certain wavelengths (optical/infrared, thermal, microwave region).

Depending on the wavelength, the electromagnetic radiation may be available from a natural source or it must be transmitted by the instrument. If the radiation is available from natural sources, the instruments are called passive. These instruments are found in the optical and thermal spectral regions and short wavelength microwave regions. Some instruments transmit radiation and measure the amount of radiation returning from the target. These instruments are called active and they can be found in the microwave region and optical/infrared region.

The usefulness of different wavelengths in forest analysis varies. The reason for this is in the interaction between the radiation and the different constituents of the forest. The most useful wavelengths are in the visible (VIS, wavelength 400-700 nm) and infrared region (near infrared NIR 700-1000 nm and, to a lesser extent, shortwave infrared SWIR 1000-2500 nm). The interaction in the microwave region is weaker.

The pixel size: The size on ground of the picture elements (pixels) produced by different sensors varies very much. The smallest pixels in current optical instruments are about 60 cm whereas the largest pixel sizes in passive microwave instruments are in the order of tens of kilometres. In some cases (e.g., passive microwave instruments) the pixel size is limited by the physics whereas in other cases (e.g., the weather satellites) the pixel size is limited by the application properties.

The ground resolution of an instrument is more difficult to define than the pixel size. For any reasonable imager the resolution is close to the pixel size and it is sufficient for this discussion to use the pixel size for characterisation of the instruments.

The most useful pixel size for forest applications depends on the information needs. The spatial units being investigated should usually include at least a small number of pixels. The number of pixels falling on the borders between the units should not be too large.

The image size grows rapidly when the pixel size is made smaller. This limits the useful resolution because the processing load must be within the economical limits set by the

application. However, one should not that the processing capability of the computers and the sizes of storage media increase rapidly. This allows use of better resolution in future if the human operating work does not grow.

The data transfer capabilities between satellites and ground stations are limited. This sets a limit to the amount of information that can be collected by a sensor in a unit of time. This means that with a smaller pixel size the area covered by the images gets smaller and the number of images needed to cover a specified are gets larger.

The radiometric characteristics: The power of the electromagnetic signal available at the sensor element of a passive instrument depends on the pixel size and the wavelength range. Active instruments add the transmitted power to this list. The radiometric (brightness) resolution in a data pixel depends also on the sensitivity of the sensor system.

In practice, the radiometric accuracy of the existing sensors can be considered adequate but, in some cases, it limits the usability of the data in some applications. For instance, the reflectivity of forest targets is low in the visible range and the radiometric resolution of a data source may limit the obtainable accuracy when using channels from the visible range. This is significant especially at high latitudes where the sun elevation is low.

Availability of the images: The availability of images from different sensors is limited by several factors. Some of these limits come from the nature and some of the factors from commercial and organisational sources.

The natural limitations are different for different wavelengths. Acquisition of the optical images is limited by the clouds. The severity of this limitation depends on the area but it is a considerable limitation for all areas with forest cover. Another limitation of the passive optical sensors is that they can operate only in daylight conditions. The elevation of the sun has effect on the usability of the images and this further limits the availability of the images.

The microwave instruments are nearly insensitive to weather conditions within the atmosphere. However, the moisture of the target affects the images strongly.

The time one satellite can collect images during one orbit may be limited by data storage capacity within the satellite, the downlink capacity, or by power conditions. Together with the pixel size, this limits the area the satellite can image within a time unit. Some satellites have a limited pointing capability and this increases the possibilities to obtain an image from a certain site if the pixel size is small. However, this off-nadir viewing affects the quality of the images.

The satellites usually acquire images based on programming (a customer orders an image covering a certain area and the satellite is tasked to do this) and as background activity (the extra instrument operating time available after specific orders is used to collect images from areas that may be used in future). The images from both acquisition types are usually archived for possible later use. The availability and the condition of these archives must be checked if a system is to use existing imagery.

In practice, the availability of images for an application may be limited by the price of images. This applies mostly to the sensors developed specifically for commercial applications (e.g., sensors with small pixel size).

Availability of images on a long-term basis is an important consideration when building a monitoring system. Continuity requirements may be fulfilled either by a series of similar instrument or by different instruments providing similar capabilities. The design life of one remote sensing satellite is typically about five years. However, a satellite may operate much longer or it may fail sooner. This is not known in advance.

In addition to radiometrically and/or geometrically corrected images, some satellite systems provide so called Level 3 image products. One example of these is the MODIS land cover product which classifies the land cover into 17 classes.

Pricing: The price of image data varies according to the instrument but also according to many other factors. These include the receiving station, geographic area, customer type, archive vs. tasking, acquisition priority, and number of images ordered. The prices given below indicate the order of magnitude of the prices of the different products when writing this document.

3.2. Sensor Classification

Classification based on pixel size is shown in Table 2. Another classification done on the basis of the information mediator is in Table 3.

Table 2: The sensor classes

	Pixel dimensions	Swath width
Low-resolution	≥ 1000 m	≥ 2000 km
Medium-resolution	100 - 1000 m	500 - 2000 km
High-resolution	10 - 30 m	50 - 200 km
Very-high resolution	≤ 5 m	5 - 20 km

Table 3: The information mediator based instrument classification

Type	**Wavelength range**	**Nbr channels (polarizations)**
Optical	Panchromatic	1
	VIS & NIR	4
	VIS & NIR	10 - 30
	VIS & NIR & SWIR	6
	VIS & NIR & SWIR	20 - 30
	VIS & NIR & SWIR	150 - 300
Microwave	C band	1
		2
		4 (polarimetric)
	L band	1
		4 (polarimetric)

Classifications for applications can be derived based on these classifications and algorithmic and system consideration. If an application requires a certain set of channels within some pixel size and swath width limits, these constraints define a class that contains one or more instruments (or none if the constraints are too tight).

A practical classification useful for predicting the availability and price level of the data comes from the purpose of the satellites. This classification divides the satellites into four classes: experimental, research, non-commercial operational, and commercial operational.

The amount of data available from experimental satellites is usually small and there is no guaranteed continuity. This data may be useful locally in some special cases.

The research satellites may be specialised or general. Some produce only a small amount of data and are useful in special cases. Some others (like NASA's MODIS and ESA's Envisat) produce large amounts of data worldwide. The price of data from the research satellites is usually low (handling costs) but the continuity of similar data after the satellite has failed is not guaranteed.

The non-commercial operational satellites (like the weather satellites and Landsat) produce large amounts of data and the continuity is good. This usually means also that there exist large archives of images from previous years. The price of data from these satellites is low because the governments are paying most of the costs.

The commercial operational satellites (e.g., Spot and the very-high resolution satellites) include the costs of the satellites and operation into the image prices. The continuity is good if the commercial demand for the image type continues.

Note that inclusion of a satellite into one of the two operational categories may depend on the nationality of the data buyer. In many cases, the buyers from countries financing the satellite are charged non-commercial price whereas others pay commercial prices.

3.3. Covering the globe with image samples

Taking into account the objective of the global survey, the price of the images and needed workload, sampling may be the only feasible way to utilise remote sensing data in the case of high and very high resolution remote sensing data. Total cover is feasible with medium resolution data, such as MODIS. Examples of required image numbers and prices are given in Table 4 with some sampling options. MODIS, Landsat ETM and Ikonos are used as examples. The price vary by region and dealer, a price of 600 US$ for Landsat ETM and 2700 US$ for Ikonos have been applied in the example. MODIS images are supposed to be charge free. The total price in the example is dominated by the Ikonos images.

Table 4: The number of the needed images estimated costs with 0.1 % and 1 % Ikonos sampling options

Region	MODIS Total cover	Landsat ETM+ 10 % cover	Ikonos 0.1 % cover	Ikonos 1 % cover	Landsat costs US $	Total costs 0,1 % Ikonos	USD 1 % Ikonos
Africa	6	97	331	3309	58008	951408	8992008
Asia	6	100	343	3428	60093	985593	9315093
Europe	4	73	251	2511	44022	722022	6824022
North and Central	4	69	237	2374	41626	682726	6452626
Oceania	2	28	94	943	16538	271238	2563538
South America	3	57	195	1950	34186	560686	5299186
Total	**25**	**424**	**1452**	**14516**	**254473**	**4173673**	**39446473**

4. Survey design cases and the evaluation of the cases

4.1. Identification of the parameters to be estimated

In a possible global survey, the key variables are areas of forest land, other wooded land and other land as well as their changes over time. Optional variables are tree stem volume and tree biomass, together with changes. Earlier remote sensing studies support the assumption that a breakdown into rough species groups should be possible by means of remote sensing aided analysis. The parameters which are possible to estimate using remote sensing aided method depend on the intensity of the field sampling. The estimation of the volume of growing stock and biomass of trees presumes a moderate field sampling intensity and measurements of tree components. There are many studies concerning the accuracy of the above mentioned variables with field measurements and remote sensing data. Rather dense field sampling grid has been applied in most studies. There is a lack of studies with very sparse field sampling intensity. The accuracy of estimates with sparse field sampling could be one topic in a possible global pilot study.

A couple of survey cases are given in the following. They are only tentative. The final error analysis needs more study and pilot studies. A method to estimate sampling error through simulation is outlined in Appendix 1. The FRA 2000 land cover map of FAO, produced by EROS Data Center has been applied in that study. Other global forest cover maps may also be available for the possible global survey. These will be very useful data sources in planning sampling designs in a similar way.

4.2. Examples of global level costs

In order to get an idea of the level of the field measurement costs and to be able to compare those with remote sensing aided surveys, a rough calculation is first given in which only field data are used. The area represented by one field plot varies here from 30 000 ha in areas with no changes to 10 000 ha with a relative annul change of 0.8 %. The total costs with these assumptions exceed USD 100 mill., and USD 10 mill. if only one tenth of the plots are applied (Table 5). The costs of images corresponding 10 % Landsat ETM+ cover together with 100 field plots per image scene are given in Table 6. Comparison of the costs of the Table 5 and Table 6 shows that field data dominate the cost.

Table 5: An example of the number and costs of field plots in a global survey utilising field data only

Region	Land area	Forest area	Net change 1990-	Net change 1990-	Area represented by one plot	Number of field plots	Estimated costs
	mill. ha	mill. ha	mill.ha/year	% / year			US $
Africa	2978	650	-5,3	-0,815	13692	69221	30457393
Asia	3085	548	-0,4	-0,073	28540	30010	13204558
Europe	2260	1039	0,9	0,087	28268	44751	19690412
North and Central America	2137	549	-0,6	-0,109	27814	27421	12065345
Oceania	849	198	-0,4	-0,202	25960	10898	4794989,9
South	1755	886	-3,7	-0,418	21648	49035	21575347
Total	**13064**	**3869**	**-9,4**	**-0,243**		**231336**	**101788045**

Table 6: Estimated costs with 100 field plots per Landsat ETM image and 440 US $ per plot

Region	Field data	Image data	Total costs
Africa	4253940	58008	4311949
Asia	4406785	60093	4466878
Europe	3228309	44022	3272332
North and Central America	3052609	41626	3094236
Oceania	1212759	16538	1229296
South America	2506939	34186	2541125
Total	**18661342**	**254473**	**18915815**

4.3. Demonstration of the standard errors in Europe and CIS

For demonstrating the behaviour of the standards errors computed with the methods given in Appendix 1, we conducted the following experiment. The area of Europe and CIS was covered with two optional Landsat ETM+ densities 1) with 150 scenes and 2) with 300 scenes. The first option is nearly the density used in tropics for FRA 1990 and FRA 2000. We assumed that a digital image analysis of one Landsat TM scene requires 5 working days. A cost of USD 600 was assumed for one Landsat scene and a cost of USD 400 for one working day. The field data costs were not included in the first two options (Table 7). In the options 3 and 4 (Table 8), the costs of 100 field plots per one Landsat scene are included, USD 44 000 per scene. The number of Ikonos scenes was computed in such a way that total costs, including the image cost and two working days for one Ikonos scene, were same as with Landsat options. Two different prices were assumed for Ikonos, 1) USD 2700 and 2) USD1000 in anticipation of a potentially more competitive market in the future.

Table 7: Two Landsat ETM+ cover options with a processing time of 5 working days per image and the number of Ikonos scenes with two price options corresponding to the same total costs as Landsat options. Ikonos is assumed to require 2 working days per scene. The cost of 400 USD has been used for one working day.

Europe & CIS	150 Landsat scenes a 600 USD	300 Landsat scenes a 600 USD
No of Landsat	150	300
costs	390000	780000
No of Ikonos scenes, a 2700 USD	111	223
No of Ikonos scenes, a 1000 USD	217	433

Table 8: Two Landsat ETM+ cover options with a processing time of 5 working days per image and the number of Ikonos scenes with two price options corresponding to the same total costs as Landsat options. Ikonos is assumed to require 2 working days per scene. The cost of 400 USD has been used for one working day. With Landsat ETM+, the costs of 100 field plots with unit costs of USD 440 have been included.

Europe & CIS	150 Landsat scenes a 600 USD	300 Landsat scenes a 600 USD
No of Landsat	150	300
costs	6990000	13980000
No of Ikonos scenes, a 2700 USD	1997	3994
No of Ikonos scenes, a 1000 USD	3883	7767

The number of Ikonos samples varies under these assumptions from n=111 to n=7767. Note that field data costs are not included in the Ikonos options. We have assumed that forest area and change in forest area can be interpreted from Ikonos or similar images without field data. The validity of this hypothesis must be tested in future analysis.

We use simulations to evaluate the feasibility of multiple-resolution remote sensing for FRA 2010 objectives. The simulation has the following components (see Appendix 1).

1. Construct a realistic hypothetical population that fully covers a very large region. The selected region was Europe and the Commonwealth of Independent States (CIS). The combined land area[1] is 2.7-billon hectares, of which 38% is forestland and another 4% is other wooded land.

[1] Europe has a total land area of 565,930,000-ha; 31% is forestland and 7% is other wooded land (FAO 2000). CIS has a total area 2,213,036,000-ha; 40% is forestland and 4% is other wooded land. Europe covers 21% of the simulation population, while CIS covers 79%.

2. Simulate changes in forest cover in this hypothetical population over a 10-year time interval.

3. Simulate estimates of forest area from satellite data with multiple resolutions (1-km, 30-m and 1-m) for the entire hypothetical population at the beginning (2000) and end of the 10-year time interval (2010).

4. Compare alternative sampling designs to statistically estimate the area of forest cover and changes in forest cover during the 10-year interval.

5. Predict the statistical precision and cost of these alternative designs for possible use by FRA 2010 in the future.

The standard errors and coefficients of variation for the estimates obtained with Landsat image analysis are given in Table 9. The corresponding errors for estimates obtained with Ikonos image interpretation with two different Ikonos image price assumptions are presented in Table 10 when field measurement costs are excluded from Landsat options, and in Table 11 when field measurement costs are included in Landsat image options. A relatively small change rate makes the coefficient of variation high for the changes of forest area in all alternatives. The error level is near acceptable in all cases.

A somewhat surprising result is that the sampling errors with much smaller Ikonos images are about at the same level as, or even smaller than, those with about same number of much larger Landsat images. This appears to be caused by methods used to reduce variability with sub-strata (Appendix 1). This technique appears more successful with smaller sampling units, at least with the hypothetical population constructed for this study.

A fact which can affect the competitiveness of high resolution and very high-resolution images is the availability of the very high-resolution images. It is much more uncertain than that of high-resolution images. The needed double coverage of images for change analysis makes the situation more complicated with high-resolution images (see conclusions and discussion).

Our simplified simulation model shows that high resolution and very high-resolution image based forest survey can meet the accuracy requirements of a possible independent remote sensing aided forest survey with a moderate cost. The final conclusions would need further analysis and more resources than what was available in this study. The procedure described here could be repeated in the other regions of the globe as well, with some other remote sensing based material, and with other variables than which were used here.

Table 9: The standard errors and coefficients of variation when Landsat images are applied

	150 Landsat scenes	300 Landsat scenes
Standard error		
Forest area time 0 (km^2)	388 587	253 377
Other Wooded land area time 0 (km^2)	42 661	28 373
Change in forest area from time 0 to time 10 (km^2)	30 100	19 365
Change in other wooded land area from time 0 to time 10 (km^2)	7 912	5 254
Rate of change in forest area %/10-years	0,38 %	0,25 %
Rate of change in other wooded land area %/10-years	0,96 %	0,65 %
Coefficient of Variation		
Forest area time 0 (km^2)	3,85 %	2,51 %
Other Wooded land area time 0 (km^2)	3,90 %	2,60 %
Change in forest area from time 0 to time 10 (km^2)	122,70 %	78,94 %
Change in other wooded land area from time 0 to time 10 (km^2)	4,94 %	3,28 %
Rate of change in forest area %/10-years	157,85 %	104,40 %
Rate of change in other wooded land area %/10-years	6,58 %	4,46 %

Table 10: The standard errors and coefficients of variation when Ikonos images are employed. Field plot costs of Landsat images are excluded

	111 Ikonos scenes	217 Ikonos scenes	223 Ikonos scenes	443 Ikonos scenes
Standard error				
Forest area time 0 (km^2)	310 644	221 359	214 476	152 643
Other wooded land area time 0 (km^2)	51 478	36 606	36 194	25 671
Change in forest area from time 0 to time 10 (km^2)	36 469	26 533	25 436	18 248
Change in other wooded land area from time 0 to time 10 (km^2)	10 817	7 791	7 629	5 441
Rate of change in forest area %/10-years	0,34 %	0,25 %	0,24 %	0,17 %
Rate of change in other wooded land area %/10-years	0,60 %	0,43 %	0,43 %	0,30 %
Coefficient of Variation				
Forest area time 0 (km^2)	3,08 %	2,19 %	2,12 %	1,51 %
Woodland area time 0 (km^2)	4,71 %	3,35 %	3,31 %	2,35 %
Change in forest area from time 0 to time 10 (km^2)	148,66 %	108,16 %	103,69 %	74,39 %
Change in other wooded land area from time 0 to time 10 (km^2)	6,75 %	4,86 %	4,76 %	3,40 %
Rate of change in forest area %/10-years	142,03 %	103,58 %	99,75 %	71,43 %
Rate of change in other wooded land area %/10-years	4,10 %	2,97 %	2,90 %	2,07 %

Table 11: The standard errors and coefficients of variation when Ikonos images are employed. The field plot costs of Landsat analysis are included

	1197 Ikonos scenes	3883 Ikonos scenes	3994 Ikonos scenes	7767 Ikonos scenes
Standard error				
Forest area time 0 (km^2)	71 972	51 381	50 695	36 194
Other wooded land area time 0 (km^2)	12 083	8 626	8 503	6 066
Change in forest area from time 0 to time 10 (km^2)	8 579	6 124	6 033	4 301
Change in other wooded land area from time 0 to time 10 (km^2)	2 549	1 820	1 795	1 279
Rate of change in forest area %/10-years	0,08 %	0,06 %	0,06 %	0,04 %
Rate of change in other wooded land area %/10-years	0,14 %	0,10 %	0,10 %	0,07 %
Coefficient of Variation				
Forest area time 0 (km^2)	0,71 %	0,51 %	0,50 %	0,36 %
Other wooded land area time 0 (km^2)	1,11 %	0,79 %	0,78 %	0,56 %
Change in forest area from time 0 to time 10 (km^2)	34,97 %	24,96 %	24,59 %	17,53 %
Change in other wooded land area from time 0 to time 10 (km^2)	1,59 %	1,14 %	1,12 %	0,80 %
Rate of change in forest area %/10-years	33,55 %	23,94 %	23,62 %	16,82 %
Rate of change in other wooded land area %/10-years	0,97 %	0,69 %	0,68 %	0,49 %

5. Conclusions and discussion

Satellite images have been successfully applied in the Forest Resource Assessment 1990 and 2000 in tropics. So far, the global wall-to-wall forest cover maps have been based on low or medium resolution images. It is expected that global wall-to-wall mapping applications with high-resolution images will appear in few years (Zhu and Walter 2001). However, this might not reduce the need for an independent remote sensing aided forest resource survey. The strength of this type of scientific survey would be the forest inventory with exact FAO definitions and estimates with current state and changes, together with standard errors, which are computed under strict quality control. A representative field sample would support this goal. Country capacity building could be an additional benefit of this type survey. Existing wall-to-wall forest cover maps could be utilised in planning the design of the survey. For a possible global survey, its role should be assessed against the existing and coming other global surveys.

The satellites launched after the FRA 1990 and FRA 2000 surveys, and new satellites under planning, increase noticeably the availability of optical area satellite images for a possible remote sensing aided survey in FRA 2010. The most interesting satellite programs are Landsat and MODIS, and possibly some programs with very high-resolution images, like Ikonos and QuickBird. Landsat 7 with the ETM+ sensor was launched in 1999. The next Landsat launch has been planned for year 2006 (Appendix 2). Imagery from Spot and IRS-1 satellites can be used for completing the image cover if Landsat images are not available, e.g., due to cloud cover. The medium resolution instruments, e.g., MODIS, MERIS and IRS-1C/D WiFS can be used for global wall-to-wall mapping. The spatial resolution for estimating changes may be problematic. The instruments have, however, good potential for planning global remote sensing and field sampling designs.

Sampling might be the only relevant approach with high-resolution images (Landsat ETM+, Spot, IRS-1 LISS-III). The number of the needed Landsat ETM+ scenes with 10 % sampling for the entire globe is about 400 - 450 and the estimated costs about 255 000 US$. The price can be compared to the costs of pure field measurement based survey. The minimum field measurement costs for this type of survey could be around 10 million US$ and likely costs around 100 million US$ (Table 5, Chapter 5).

The operational use of satellite images in forest inventories began about ten years ago, in spite of the fact that satellite image research has been active almost 30 years. The progress in estimation, error estimation method and image analysis methods can be utilised in the survey.

The main emphases in our study are 1) outlining how the evaluation of a sampling design in a remote sensing based survey could be accomplished and 2) presenting rough error estimates for the variables 'Area of Forest land' and 'Area of Other wooded land' in our test area (Europe and CIS). A hypothetical simulation model based on FRA 2000 land cover map was applied. Our study shows promising results in the applied test area, e.g., high resolution and very high resolution image based forest survey can meet the accuracy requirements of a possible independent remote sensing aided forest survey with a moderate costs. The final conclusions will need further analysis and more resources than what was available in this study. The procedure described here could be repeated in the other regions of the globe as well, with

some other remote sensing based material, and with some other variables than which were used here.

One fact which should be taken into account in planning the remote sensing based survey is the availability of satellites images from an earlier time point, particularly if very high resolution satellite images will be used. Very high-resolution images are not necessarily archived and the images are taken only upon request. There are two different options to handle this problem, 1) either to order the image from time 0 early enough, or 2) to develop a multi-resolution technique for change detection part (which can, of course, be also utilised in analysing the current status). The early order presumes fast decisions and might be unrealistic taking into account the current status of very high-resolution satellites. Thus the option 2 in which high resolution images are acquired from time 0 and very high resolution together with high-resolution images are acquired from time 10 may be a more realistic option.

The existing and upcoming medium resolution satellite images, in addition to existing and coming wall-to-wall land cover maps, provide information sources for planning both a possible field measurement based and remote sensing based sampling designs. Based on this fact and our experiment, we are convinced that an independent remote sensing aided global forest survey could be carried out with reasonable costs. We are also convinced that this type of inventory would have its role both in independently testing the accuracy of estimates obtained from other sources and in country capacity building.

References

Berk, A., Berstein, L. S. & Robertson, D. C. 1989. *MODTRAN a Moderate Resolution Model for LOWTRAN 7,* Air Force Geophysics Laboratory, AFGL-TR-89-0122, Hanscom AFB, MA 01731, April, 1989.

Czaplewski, R. 2002. *On sampling for estimating global tropical deforestation*. 2002. Forest Resource Assessment Programme.Working Paper 60. FAO. Rome 2002. (http://www.fao.org/forestry/fo/fra/index.jsp)

Drigo, R. 2002**.** *Trends and patterns of Tropical land use change*. Manuscript. FAO, Rome.

FAO 1996. Forest Resource Assessment 1990. *Survey of tropical forest cover and study of change process*. Forestry Paper No. 130. Rome.

FAO 2000. *Global Forest Survey, Concept Paper. 2000.* Forest Resource Assessment Programme.Working Paper 28. FAO. Rome 2000. (http://www.fao.org/forestry/fo/fra/index.jsp)

FAO 2001 a**.** Global Forest Resource Assessment 2000. Main Report. Forestry Paper 140. FAO, Rome. ISSN 0258-6150. (http://www.fao.org/forestry/fo/fra/main/index.jsp).

FAO 2001 b. *Pan-Tropical Survey of Forest Cover Changes 1980-2000*. FAO FRA 2000 Working Paper 49. FAO. Rome. (http://www.fao.org/forestry/fo/fra/index.jsp).

Franco-Lopez, H., Ek, A.R., & Bauer, M. E., 2001. *Estimation and mapping of forest stand density, volume and cover type using the k-nearest neighbors method*. Remote Sensing of Environment, 77, 251-274.

Katila, M., Heikkinen, J., & Tomppo, E. 2000. *Calibration of small-area estimates for map errors in multisource forest inventory*. Canadian Journal of Forest Research, 30, 1329-1339.

Katila, M. & Tomppo, E. 2002**.** *Small area estimates for multi-source forest inventory by strata*. Canadian Journal of Forest Research. In press.

McRoberts, E. Nelson, M. D., & Wendt, D. G. 2002**.** *Stratified estimation of forest area using satellite imagery, inventory data, and the k-Nearest Neighbors Remote Sensing of Environment 2002*. In press.

Nilsson, M. 1997. *Estimation of Forest Variables Using Satellite Image Data and Airborne Lidar*. PhD thesis. Swedish University of Agricultural Sciences, The Department of Forest Resource Management and Geomatics, Acta Universitatis Agriculturae Suecica. Silvestria 17.

Poso, S., Wang, G. and Tuominen, S., 1999. *Weighting Alternative Estimates when Using Multi-Source Auxiliary Data for Forest Inventory.* Silva Fennica 33 (1), 41-50.

Stokstad, E. 2001**.** U.N. *Report suggests slowed forest losses*. Science 291, 2294.

Tokola, T., Pitkänen, J., *et al*. 1996**.** *Point accuracy of a non-parametric method in estimation of forest characteristics with different satellite materials.* International Journal of Remote Sensing, 17, 2333-2351.

Tomppo, E. 1990. *Designing a Satellite Image-Aided National Forest Survey in Finland*. The Usability of Remote Sensing for Forest Inventory and Planning. Proceedings from SNS/IUFRO workshop, 26-28 February, 1990 (pp. 43-47) Umeå, Sweden.

Tomppo, E. 1996. *Multi-source National Forest Inventory of Finland*. In: R. Vanclay, J. Vanclay, & S. Miina (Eds.) New Thrusts in Forest Inventory. Proceedings of the Subject Group S4.02-00 'Forest Resource Inventory and Monitoring' and Subject Group S4.12-00 'Remote Sensing Technology'. Volume 1. IUFRO XX World Congress 6-12 August 1995 (pp. 27-41) Tampere, Finland. EFI Proceedings No. 7. 15 pp. European Forest Institute. Joensuu, Finland.

Tomppo, E., Nilsson, *et al*. 2002**.** *The co-use of Landsat-TM and IRS-1C WiFS data in estimating Large Area Tree Stem Volume and Above-Ground Biomass*. Remote Sensing of Environment. In press.

Tomppo, E. & Halme, M. 2002**.** *Selecting weights of satellite image and ancillary information in k-nn estimation - a genetic algorithm approach*. Manuscript. Finnish Forest research Institute.

Vermote, E. F.,Tanré, D. *et al*. 1997**.** *Second simulation of the satellite signal in the solar spectrum, an overview.* IEEE Transactions on Geoscience and Remote Sensing. 35(3): 675-686.

Zhu, Z. & E. Walter. 2001**.** *Global forest cover mapping*. FRA Working Paper No. 50. Rome. 29pp.

Appendix 1: Simulation study for Europe and CIS

by

Raymond L. Czaplewski and Erkki Tomppo

FRA 2010 will consider the following issues and assessment questions:

1. Biodiversity, climate change, desertification, carbon cycling
2. International economic analyses and forecasting
3. Current extent and condition of forests globally
4. Rapid changes in forest cover and land use, deforestation
    a. How much forest is being lost? Gained?
    b. Where is forest being lost? Hot spots of deforestation and degradation
    c. What are the processes driving rapid changes
        i. Land use change, agriculture, urban
        ii. Timber harvest
        iii. Catastrophic fire, floods
5. Comparisons across different spatial scales among:
    a. Broad ecological zones across all continents
    b. Broad ecological zones within individual continents
    c. Individual countries

This FRA 2010 assessment requires a database of reliable information on the current status of forests, changes in forests between 2000 and 2010, and trends in rates of change over a longer span of time. The database needs information for broad ecological zones within individual continents, which can be grouped into broader geographic regions.

National data presents problems for global assessments at these broad, multinational scales. There are differences among nations in definitions, completeness and timeliness of their national data, even in the developed world (FAO 2000, 2001). In the tropical zone, FRA has supplemented national data with a remote sensing survey that can independently test the accuracy of national data for international analyses (FAO 2001). This survey uses internationally consistent definitions and protocols, which is not the case with all national data.

Remote sensing has its own set of challenges for global analyses. The first complete and acceptably accurate thematic map of global forest cover was first produced in the late 1990's (Loveland, 1999). This map used AVHRR satellite data, which has a spatial resolution of 1-km. However, this coarse scale introduces errors in characterizing the current status of forest cover (Moody and Woodcock 1994), and the changes in forest cover over time.

Landsat satellite data, with 30-m resolution, provide more accurate information on forest cover than AVHRR or MODIS because the spatial resolution is 100-to 1000-times greater. However, the processing burden is approximately 100- to 1000-times greater also. Land cover mapping with Landsat data for the entire the world has not yet been achieved, although there are impressive efforts underway to accomplish this massive task in the future. Measuring changes in forest cover over time (e.g., 1980, 1990, 2000, 2010) with full global coverage of Landsat data is even a larger task. A short-term alternative to full Landsat global coverage is

sampling of Landsat scenes. This was first accomplished by FAO in FRA 1990 for the tropical forested zones of the world, with a detailed analysis of changes between 1980 and 1990. In 2001, FRA 2000 produced the first global assessment of changes and trends forest cover between 1980 to 1990, and 1990 to 2000.

Remote sensing technologies have improved significantly since FRA 1990. MODIS data are now available globally at 250-m nadir resolution with much greater spectral resolution than AVHRR. MODIS offers the promise for much better global data compared to AVHRR. IKONOS satellite data have recently become available for the entire world. This and similar commercial satellites offer 1-m resolution, which is similar to high-altitude aerial photography. However, the volume of data needed for full coverage of the world increases another 1000-times relative to Landsat data at 30-m resolution.

The objective of this study is to evaluate the feasibility to improve the FRA 2010 global forest assessment using these new sources of remotely sensed data. Assumptions include:

1. Land cover mapping with full global coverage of the world with coarse resolution satellite data (250-m to 1-km pixels) will improve. This will be accomplished through institutions and programs external to FAO.

2. Consistent land cover mapping with full global coverage of the world with high-resolution satellite data (30-m resolution) will be achieved by 2010 through institutions and programs external to FAO. However, measurement of change in forest cover requires imagery from multiple dates, such as 1980, 1990, 2000 and 2010. It is assumed that full coverage with 30-m satellite data for this time series will not be accomplished by 2010. Therefore, sampling of Landsat scenes for assessments of changes and trends in forest cover will remain relevant for FRA 2010.

3. Very high-resolution satellite data (1-m resolution) can improve accuracy of the FRA 2010 database relative to classifications with 30-m resolution data. This same imagery could provide the statistical linkage between global collection of field data for FRA 2010 and an independent remote sensing survey of the world.

This study uses simulations to evaluate the feasibility of multiple-resolution remote sensing for FRA 2010 objectives. The simulation has several components.

1. Construct a realistic hypothetical population that fully covers a very large region. The selected region was Europe and the Commonwealth of Independent States (CIS). The combined land area[2] is 2.7-billon hectares, of which 38% is forestland and another 4% is other wooded land.

2. Simulate changes in forest cover in this hypothetical population over a 10-year time interval.

3. Simulate estimates of forest area from satellite data with multiple resolutions (1-km, 30-m and 1-m) for the entire hypothetical population at the beginning (2000) and end of the 10-year time interval (2010).

[2] Europe has a total land area of 565,930,000-ha; 31% is forestland and 7% is other wooded land (FAO 2000). CIS has a total area 2,213,036,000-ha; 40% is forestland and 4% is other wooded land. Europe covers 21% of the hypothetical population, while CIS covers 79%.

4. Compare alternative sampling designs to statistically estimate the area of forest cover and changes in forest cover during the 10-year interval.

Predict the statistical precision and cost of these alternative designs for possible use by FRA 2010 in the future

Methods

Construction of a hypothetical population

Full coverage with realistic landscape patterns

The hypothetical population mimics Europe and CIS. This geographic area is composed of ten major ecological zones (Figure 2).

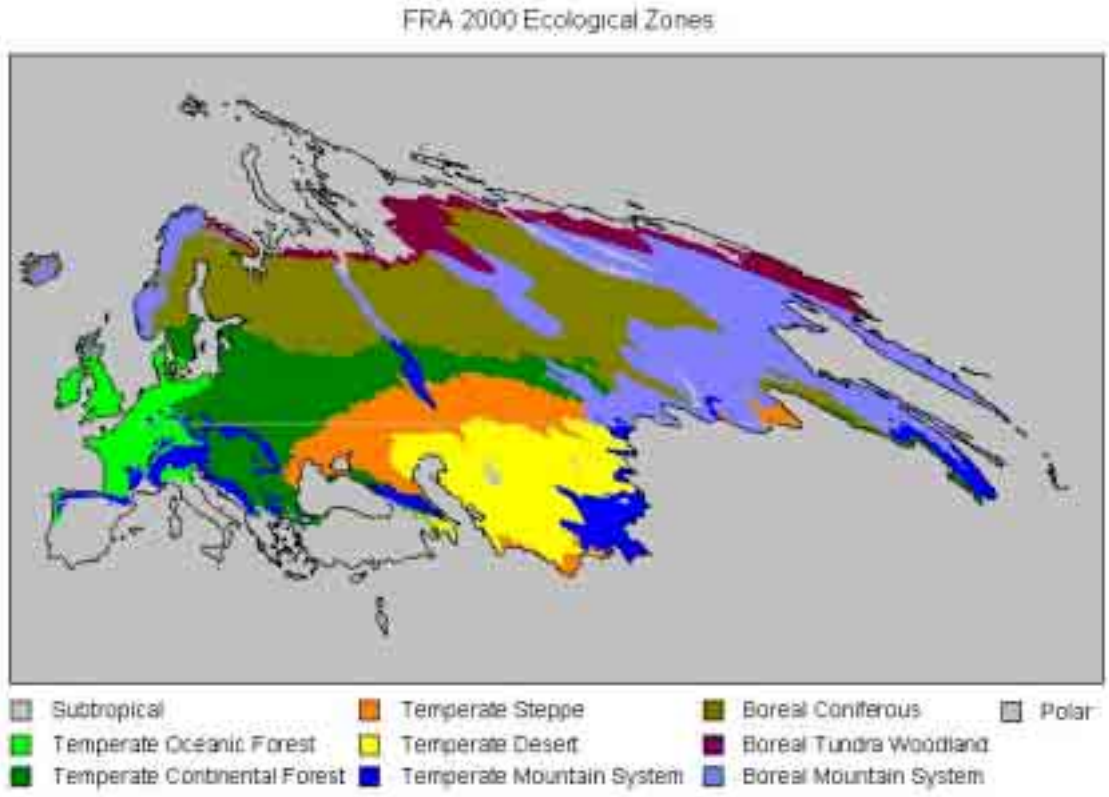

Figure 2: FRA 2000 ecological zones for Europe and CIS (2,268,966-km^2).

The statistical efficiencies of alternative sampling designs are affected by the detailed spatial structure of regional and local landscape patterns within a population. The FRA 2000 global forest cover map (FAO 2001) for Europe and CIS was used to add this spatial realism into the hypothetical population. The FRA 2000 map uses 1-km cells classified into one of five categories (Table 12). This map is a modification (Zhu and Waller 2001) of the Global Land Cover Characteristics Database (Loveland et al. 1999) produced by the USGS Eros Data Center.

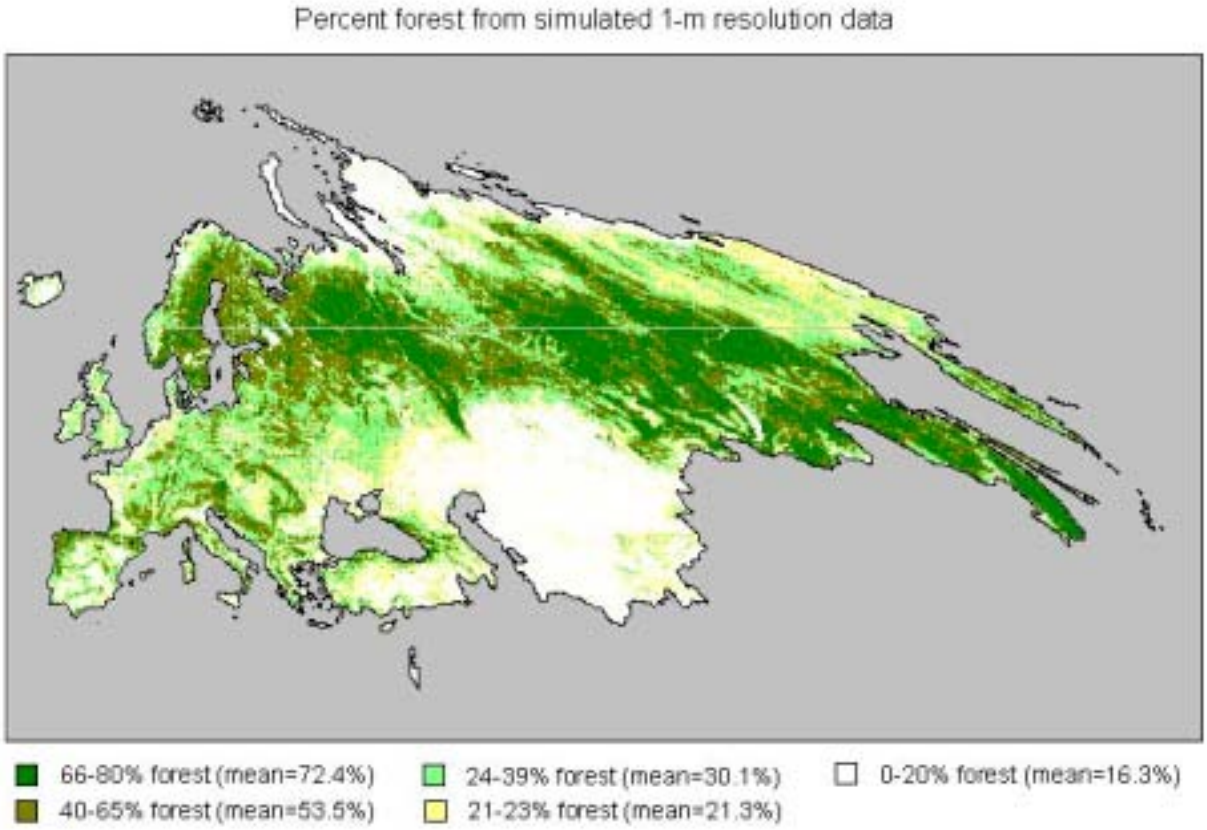

Figure 3: FRA 2000 global forest cover map. The spatial resolution is 1-km, and contains five categories of forest and other cover (Table 12).

Table 12: FRA 2000 global land cover map legend, definitions and representative land cover types (FAO 2001). Figure 2 gives a broad perspective of this map for Europe and CIS. The spatial resolution is 1-km.

FRA 2000 class	FAO definition	Representative land cover
Closed forest	Land covered by trees with a canopy cover of more than 40 percent and height exceeding 5 m. Includes natural forests and forest plantations.	Temperate broadleaf mixed forest Subtropical/temperate conifer plantation Boreal conifer forest
Open or fragmented forest	Land covered by trees with a canopy cover between 10 and 40 percent and height exceeding 5 m (open forest), or mosaics of forest and nonforest land (fragmented forest). Includes natural forests and forest plantations.	Northern boreal/taiga open conifer or mixed forest
Other wooded land	Land either with a 5 to 10 percent canopy cover of trees exceeding 5 m height, or with a shrub or bush cover of more than 10 percent and height less than 5 m.	Mediterranean closed shrubland
Other land cover	All other land, including grassland, agricultural land, barren land, urban areas.	Grassland, cropland, non-woody wetland, desert, urban
Water	Inland water.	Inland water.

Alternative sampling frames

The hypothetical population[3] is divided into two alternative area sampling frames. The first frame uses a 150x150-km Large Sampling Unit (LSU), which is defined as approximately the average size of a non-overlapping Landsat scene at higher latitudes. There are a total of 1627 LSUs (i.e., simulated Landsat scenes) in Europe and CIS. However, 152 LSUs are covered by at least 90% ocean and large water bodies. These are excluded from the sampled population to reduce cost and variance. A total of 1473 LSUs are available for sampling.

The second sampling frame uses a 10x10-km Small Sampling Unit (SSU), which is approximately the field of view for a 1-m resolution image (e.g., IKONOS). There are 284,760 SSUs in the hypothetical population. However, 2265 SSUs are covered with at least 90% ocean or large water bodies, and are excluded from the sampled population. A total of 282,495 SSUs are available for sampling, although only a fraction of these units are actually included in any one sample.

The percent of each land cover category (Table 12) was computed from the FRA 2000 global map (similar to Figure 3)for each simulated LSU and SSU. These percentages simulate future results from a global classification with MODIS data, where MODIS could be used to estimate the proportion of each land cover category in each SSU. This is a pessimistic simulation because MODIS is expected to be more accurate for land cover mapping than AVHRR, and the realized results for FRA 2010 should be somewhat better than predicted by this simulation.

[3] This hypothetical population is approximately the same size and general composition as the global tropics, which was studied by FRA with a sample of 117 Landsat scenes (FAO 2001).

Simulated Landsat data

For statistical estimation purposes in FRA 2010, Landsat could be used to estimate the percentages of each category of land cover in a LSU or SSU. Statistical simulations require known values for all sampling units in the hypothetical population. Classification of each Landsat scene was simulated for the hypothetical population with a statistical calibration procedure, and only the simulated area statistics stored in the simulation database. The database for the hypothetical population stored the following fields for each of the 284,760 simulated SSUs (and the corresponding 1,627 LSUs):

Table 13: Data base used in sampling simulations (284,760 records)

Latitude, Longitude	
Identification number for 150x150-km PSU	
Identification number for 10x10-km SSU	
FRA 2000 Ecological Zone code (10 major zones)	
Country code	
Total area of SSU (approximately 100-km^2)	
Area (km^2) of large inland water bodies, ocean, and other non-land types	
Time 0	Area (km^2) from FRA 2000 global forest cover map (FAO 2001), with 1x1-km pixels 1. Closed Forest (60-100% forest in 1-km pixel) 2. Open and Fragmented Forest (30-60% forest in 1-km pixel) [§] 3. Other Wooded Land 4. Other Land Cover (includes small inland water bodies)
	Simulated area (km^2) expected from classification of 30-m resolution Landsat data using calibration model from 1-km to 30-m resolution. Inputs to the calibration model are the area statistics at time t=0 from fields 1 to 4 at Time 0. 5. Forest 6. Other Wooded Land 7. Other Land Cover (includes small inland water bodies)
	Simulated area (km^2) expected from classification of 1-m resolution Ikonos data using calibration model from 30-m to 1-m resolution. Inputs to the calibration model are the area statistics at time t=0 from fields 5 to 6 at Time 0. 8. Forest 9. Other Wooded Land 10. Other Land Cover (includes small inland water bodies)
Time +10	Simulated area (km^2) from FRA 2000 global forest cover map using change transition matrix (unique to each individual SSU) using fields 1 to 4 at Time 0. 11. Closed Forest (60-100% forest in 1-km pixel) 12. Open and Fragmented Forest (30-60% forest in 1-km pixel) [§] 13. Other Wooded Land 14. Other Land Cover (includes small inland water bodies)
	Simulated area (km^2) expected from classification of 30-m resolution Landsat data using calibration model from 1-km to 30-m resolution. Inputs to the calibration model are the area statistics at time t+10 from fields 11 to 14. 15. Forest 16. Other Wooded Land 17. Other Land Cover (includes small inland water bodies)
	Simulated area (km^2) expected from classification of 1-m resolution Ikonos data using calibration model from 30-m to 1-m resolution. Inputs to the calibration model are the area statistics at time t+10 from fields 15 to 17.
	18. Forest 19. Other Wooded Land 20. Other Land Cover (includes small inland water bodies)
	[§]The area of "Open and Fragmented Forest" (30-60% forest in 1-km pixel) exists only at the 1-km resolution of the FRA 2000 global forest cover map. Such areas are considered mosaics, which are composed of more specific categories (i.e., Forest, Wooded, and Other Land Cover). These mosaics are classified into the specific categories (i.e., Forest, Wooded, and Other Land Cover) with the simulated 30-m and 1-m resolution remotely sensed data.

The basis for this statistical procedure is the error matrix (Scepan 1999), also known as an "confusion matrix", that was produced for the Global Land Cover Characteristics Database (Loveland et al. 1999). This map is the primary source for the FRA 2000 global land cover map (Zhu and Walter 2001).

5. Landsat data were simulated for each SSU using the data from the FRA 2000 global land cover map (Zhu and Walter 2001). These data formed the basis of a multivariate calibration model (Czaplewski 1992) that predicts the proportional distribution of Landsat classifications for 30-m pixels as a function of classifications from the 1-km pixels in the FRA global land cover map. This model is given in Table 14A. The model is expressed as conditional probabilities in a probability transition matrix. For example, 65/78=83.33% of the Landsat pixels are expected to be classified as "Closed forest" in a 1-km global map pixel, given that the 1-km pixel is classified as "Closed forest" on the global map (Table 14).

6.

7.

8.

Table 15 gives an example that applies the calibration model for one of the 284,760 SSUs in the hypothetical population.

This calibration model is applied separately to each SSU in the hypothetical population using the unique distribution of global map classes for each SSU. This is an attempt to capture the spatial variability and error structure that exists in the real-world population. It cannot be known how well this simulates the actual spatial variability in the true population. The assumption is that the hypothetical population is sufficiently realistic for simulations and survey planning. FRA 2010 will use real data, not these simulated data, to produce the 2010 global assessment.

Table 14: Global accuracy assessment results for the FRA global land cover map (Zhu and Waller 2001) and derivation of the misclassification calibration model to simulate Landsat classifications.

A. Accuracy assessment results for FRA 2000

Global Map classification	Landsat class: Closed forest	Open or fragmented forest	Other wooded land	Other land cover	Water	Total sample points
Closed forest	**65**	2	3	8		78
Open or fragmented forest	13	**9**	3	17		42
Other wooded land	1	2	**6**	10		19
Other land cover	3	8	2	**160**		173
Water[4]					0	0
	82	21	14	195		312

B. Distribution of "Open or Fragmented Forest" at 1-km resolution into Closed Forest (45%), Other Woodland (30%) and Other Land (25%) at 30-m Landsat resolution. These distributions are assumptions used to construct the hypothetical simulation population, and they are not based on data.

Global Map classification						
Closed forest	**65.90**		3.60	8.50		78
Open or fragmented forest	17.05		5.70	19.25		42
Other wooded land	1.90		**6.60**	10.50		19
Other land cover	6.60		4.40	**162.00**		173
Total	91.45		20.30	200.25	**0**	312

Derived misclassification calibration model used to simulate Landsat classifications. This model is computed from Table 14A and applied to all 284,760 SSUs in the hypothetical population.

C. Table 15 gives an example of the calibration model applied to a single SSU.

Global Map classification						
Closed forest	**89.6%**		2.5%	7.9%	0	100%
Open or fragmented forest	51.4%		8.8%	39.8%	0	100%
Other wooded land	15.2%		**27.1%**	57.7%	0	100%
Other land cover	5.5%		1.9%	**92.6%**	0	100%
Water[5]	0		0	0	**100%**	100%

[4] The global accuracy assessment did not consider the water class.

[5] For proposes of this simulation, the water class in the global map is assumed to contain no Landsat pixels that are water bodies because accuracy assessment data are not available.

Table 15: Example showing application of the calibration model from Table 14 to simulate classification distribution of 30-m Landsat pixels within a single 10x10-km SSU, using the classification distribution of 1-km pixels from the FRA 2000 global land cover map within the same SSU

Classification of 1-km pixels in the single 10x10-km SSU from the global land cover map	Number of 1-km pixels in the SSU	Total Number of simulated 30-m Landsat pixels	Simulated distribution of 30-m Landsat pixels					Distribution of simulated MODIS pixels
			Closed forest	Open or fragmented forest	Other wooded land	Other land cover	Water	
Closed forest	30	33334	29852	0	838	2644	0	30%
Open or fragmented forest	55	61111	31386	0	5392	24333	0	55%
Other wooded land	1	1111	169	0	301	641	0	1%
Other land cover	9	10000	550	0	188	9262	0	9%
Water	5	5555	0	0	0	0	5555	5%
Total	100	111111						100%
Simulated number of Landsat pixels in SSU			61956	0	6720	36880	5555	111111
Distribution of simulated Landsat pixels			55.8%	0%	6.0%	33.2%	5%	100%

Simulated IKONOS data

This simulation considers the possibility of using 1-m IKONOS imagery to improve FRA 2010 relative to FRA 2000. 284,760 IKONOS images are be required to fully cover the hypothetical population for Europe and CIS. These images include over 10^{13} 1-m pixels. In practice, the cost of acquiring and processing such a large number of images precludes full coverage. However, a small sample of IKONOS imagery for FRA 2010 is feasible.

Just as simulated Landsat data are needed for all 284,760 SSUs in the hypothetical population, simulated classification data are needed for the same number of IKONOS images. Accuracy assessment data for the National Land Cover Dataset for the USA was used to select parameters in the calibration model (Table 16).

Table 16: Calibration model that simulates classification data from IKONOS using simulated Landsat classifications for 10x10-km SSUs. This model is applied to all 284,760 SSUs in the hypothetical population.

		Simulated IKONOS classification with photo-interpretation				
		Closed forest	Other wooded land	Other land cover	Large water bodies	
Simulated digital Landsat classification	Closed forest	**82.8%**	3.0%	14.2%	0%	100%
	Other wooded land	12.0%	**58.0%**	30.0%	0%	100%
	Other land cover	16.9%	6.0%	**77.2%**	0%	100%
	Large water bodies	0%	0%	0%	**100%**	100%

Table 17: Example showing application of the calibration model from Table 16 to simulate the classification distribution of 1-m IKONOS pixels within a single 10x10-km SSU, using the classification distribution of simulated 30-km pixels from Table 15

			Simulated distribution of 1-m IKONOS pixels					
Simulated classification of 30-m Landsat pixels in the single 10x10-km SSU	Total number of simulated 30-m Landsat pixels	Distributor of simulated 30-m Landsat pixels	Closed forest	Open or fragmented forest	Other wooded land	Other land cover	Water	Total
Closed forest	61956	55.8%	46169166	0	1659164	7932180	0	
Open or fragmented forest	0	0%	0	0	0	0	0	
Other wooded land	6720	6.0%	725726	0	3507677	1814316	0	
Other land cover	36880	33.2%	5597991	0	1974915	25618780	0	
Water	5555	5.00%	0	0	0	0	500000	
Total	111111	100.00%	52492883	0	7141755	35365276	500000	100000000
Distribution of simulated IKONOS pixels			52.5%	0%	7.1%	35.4%	5.0%	100.00%

Simulation of changes over 10 years

A primary objective of FRA is estimation of changes in forest cover between decadal assessments. Therefore, a useful simulation must include a component of change. Change was imposed on this hypothetical population through a probability transition matrix, which is similar to the calibration models used above. A transition matrix is composed of the conditional probabilities that a land cover type at time 0 will transition into the same or different cover type at time 10. FRA 2000 estimated such transition matrices for the tropics; however, similar matrices for Europe and CIS are not known. Table 18 is one attempt to create transition matrices that roughly correspond to the net changes estimated for Europe and CIS in FRA 2000. The pattern of change among land cover categories is intended to mimic steady state transitions plus human-induced changes (i.e., variable *X* in Table 18) that vary spatially.

Table 18: Change transition matrix from time 0 to time 10, applied to classes from 1-km FRA 2000 global land cover map

	Time 10				
Time 0	Closed forest	Open Frag. forest	Other wooded land	Other land cover	
Closed forest (60-100% forest)	0.985-(*X**0.9)	*X**0.2+0.005	*X**0.3+0.005	*X**0.4+0.005	100%
Open/fragmented (30-60% forest)	0.010	0.98*(1-*X*)	0.005+0.98**X**0.5	0.005+0.98**X**0.5	100%
Other wooded land	0.020	0.120	0.800	0.060	100%
Other land cover	0.020	0.080	0.030	0.870	100%
Percent reduction forest cover =*X*	0<*X*<1				

The value for *X* in Table 18 for each SSU varies according to a spatial "change risk" model, which is designed to have realistic spatial variability and result in realistic changes over a 10-year period. There are several multiplicative factors that affect the value of *X*.

The first factor in the change risk model (X_1) considers the distribution of closed forest and open/fragmented forest within a 50-km radius of the SSU. The assumption is that landscapes of this size that are almost entirely forested (80-100% closed forest) have relatively little exposure to land use changes and land clearing. However, the risk of change is assumed to be relatively high for landscapes that have more open and fragmented forest (e.g., 10-60%) intermingled with significant amounts of closed forest (e.g., 30-70%). As the amount of closed, open and fragmented forest become small in a landscape, then the rate of change in forest cover is assumed to be relative small.

Table 19: Relative index ($0 \leq X_1 \leq 1$) for change risk as a function of landscape patterns within 50-km of a 10x10-km Small Sampling Unit (SSU).

		Percent closed forest within a 50-km radius from the SSU									
		0-10%	10-20%	20-30%	30-40%	40-50%	50-60%	60-70%	70-80%	80-90%	90-100
Percent open and fragmented forest within a 50-km radius from the SSU	70-75%	0.12	0.51	0.90	0	0	0	0	0	0	0
	60-70%	0.06	0.36	0.75	1.00	0	0	0	0	0	0
	50-60%	0	0.30	0.60	1.00	1.00	0	0	0	0	0
	40-50%	0	0.15	0.45	0.90	1.00	1.00	0	0	0	0
	30-40%	0	0	0.30	0.75	1.00	1.00	1.00	0	0	0
	20-30%	0	0	0.15	0.60	1.00	1.00	1.00	0.60	0	0
	10-20%	0	0	0	0.51	1.00	1.00	1.00	0.45	0	0
	0-10%	0	0	0	0.39	0.96	1.00	0.75	0.21	0	0

The second factor in the change risk model (X_2) considers the distribution of closed forest and open/fragmented forest within each 10x10-km SSU. This is a much less expansive landscape than considered in the first factor (X_1) above. However, similar assumptions are used to assign a risk of change based on the distribution of closed forest and open/fragmented forest in the SSU (Table 20).

Table 20: Relative index ($0 \leq X_2 \leq 1$) for changes in forest cover as a function of composition within a given 10x10-km SSU.

Percent open and fragmented forest within the SSU	Percent closed forest within the SSU									
	0-10%	10-20%	20-30%	30-40%	40-50%	50-60%	60-70%	70-80%	80-90%	90-100
90-100	0.50	0	0	0	0	0	0	0	0	0
80-90%	0.48	0.6	0	0	0	0	0	0	0	0
70-80%	0.44	0.57	0.7	0	0	0	0	0	0	0
60-70%	0.42	0.52	0.65	0.80	0	0	0	0	0	0
50-60%	0.40	0.50	0.60	0.75	0.90	0	0	0	0	0
40-50%	0.35	0.45	0.55	0.70	0.87	1.00	0	0	0	0
30-40%	0.30	0.40	0.50	0.65	0.82	0.90	0.80	0	0	0
20-30%	0.25	0.30	0.45	0.6	0.80	0.95	0.75	0.60	0	0
10-20%	0.17	0.20	0.40	0.57	0.77	0.90	0.70	0.55	0.40	0
0-10%	0.10	0.15	0.35	0.53	0.72	0.85	0.65	0.47	0.35	0.20

The third factor in the change risk model (X_3) considers different risks for different ecological zones. Again, there is little data available to fit such models. The factors in Table 21 are merely assumptions for the hypothetical population.

Table 21: Change risk factor (X_3) for each ecological zone

Ecological Zone	X_3	Ecological Zone	X_3
Temperate oceanic forest	0.6	Subtropical humid forest	0.5
Temperate continental forest	0.5	Subtropical dry forest	0.7
Temperate steppe	0.7	Subtropical steppe	0.0
Temperate desert	0.0	Subtropical desert	0.0
Temperate mountain system	0.2	Subtropical mountain system	0.3
Boreal coniferous forest	0.5	Subtropical humid forest	0.5
Boreal tundra woodland	0.2		
Boreal mountain system	0.1		
Polar	0.0		

The fourth and final factor in the change risk model (X_4) considers differences among individual countries. The factors in Table 22 were chosen so that the total change by country in the hypothetical population approximately agrees with national statistics reported by FRA 2000.

Table 22: Change risk factors (X_4) for each country to mimic net changes reported by FRA 2000.

Country	X_4	Country	X_4	Country	X_4

Albania	1.00	Germany	0.40	Portugal	0.00
Armenia	0.20	Greece	0.00	Republic of Moldova	0.90
Austria	0.00	Hungary	0.60	Romania	0.60
Azerbaijan	0.10	Iceland	0.00	Russian Federation	1.00
Belarus	0.10	Ireland	0.00	Slovakia	0.05
Belgium	0.90	Italy	0.40	Slovenia	0.00
Bosnia and Herzegovina	0.15	Kazakhstan	0.10	Spain	0.10
Bulgaria	0.20	Kyrgyzstan	0.10	Sweden	0.10
Croatia	0.20	Latvia	0.00	Switzerland	0.50
Cyprus	0.20	Liechtenstein	0.00	Tajikistan	0.90
Czech Republic	0.60	Lithuania	0.20	The FYR of Macedonia	0.90
Denmark	0.80	Luxembourg	0.10	Turkey	0.90
Estonia	0.00	Malta	0.20	Turkmenistan	0.60
Finland	0.05	Netherlands	0.30	Ukraine	0.80
France	0.10	Norway	0.10	United Kingdom	0.10
Georgia	0.40	Poland	1.00	Uzbekistan	0.60
				Yugoslavia	0.90

The final change model for each individual SSU_i uses $X_i=X_1*X_2*X_3*X_4$ for that SSU with the transition probabilities from Table 18 to simulate 1-km resolution data at time 10. These estimates are then used with the calibration model in Table 14 to simulate 30-m Landsat data at time 10 for each SSU, and those simulated Landsat data at time 10 are input into the calibration model in Table 16 to simulate 1-m Ikonos data at time 10 for each SSU. Figure 4 shows the spatial distribution of change in the hypothetical population.

Table 23: Statistical summary for hypothetical population by Ecological Zone at time 0, and changes between times 0 and 10

Ecological zone	Total area (km^2)	Data source	Forest at time 0 (km^2)	Change in forest over 10-years (km^2)	Change in forest over 10 years
Subtropical	1,749,103	AVHRR	540,171	42,761	7.92%
		Landsat	366,763	60,933	16.61%
		Ikonos	531,887	40,334	7.58%
Temperate oceanic forest	1,243,743	AVHRR	421,814	28,274	6.70%
		Landsat	312,545	40,165	12.85%
		Ikonos	413,448	26,160	6.33%
Temperate continental forest	3,639,242	AVHRR	1,466,846	8,380	0.57%
		Landsat	1,325,990	2,867	0.22%
		Ikonos	1,479,238	964	0.07%
Temperate steppe	2,112,952	AVHRR	467,237	67,506	14.45%
		Landsat	220,972	99,632	45.09%
		Ikonos	496,868	66,238	13.33%
Temperate desert	2,456,317	AVHRR	459,297	-12,836	-2.79%
		Landsat	143,249	0	0.00%
		Ikonos	502,269	3,838	0.76%
Temperate mountain system	1,391,327	AVHRR	612,993	17,740	2.89%
		Landsat	590,866	24,522	4.15%
		Ikonos	621,190	16,002	2.58%
Boreal coniferous forest	5,866,169	AVHRR	3,673,218	-190,637	-5.19%
		Landsat	4,050,198	-290,480	-7.17%
		Ikonos	3,649,235	-194,697	-5.34%
Boreal tundra woodland	1,331,279	AVHRR	416,959	32,159	7.71%
		Landsat	307,694	45,120	14.66%
		Ikonos	424,360	29,324	6.91%
Boreal mountain system	4,914,168	AVHRR	2,542,564	33,676	1.32%
		Landsat	2,597,905	42,762	1.65%
		Ikonos	2,529,359	27,684	1.09%
Polar	1,895,919	AVHRR	460,565	-8,871	-1.93%
		Landsat	179,772	0	0.00%
		Ikonos	433,447	1,477	0.34%
Total for Europe and CIS	26,600,219	AVHRR	11,091,219	17,442	0.16%
	1,749,103	Landsat	10,103,675	25,521	0.25%
		Ikonos	11,093,925	17,362	0.16%

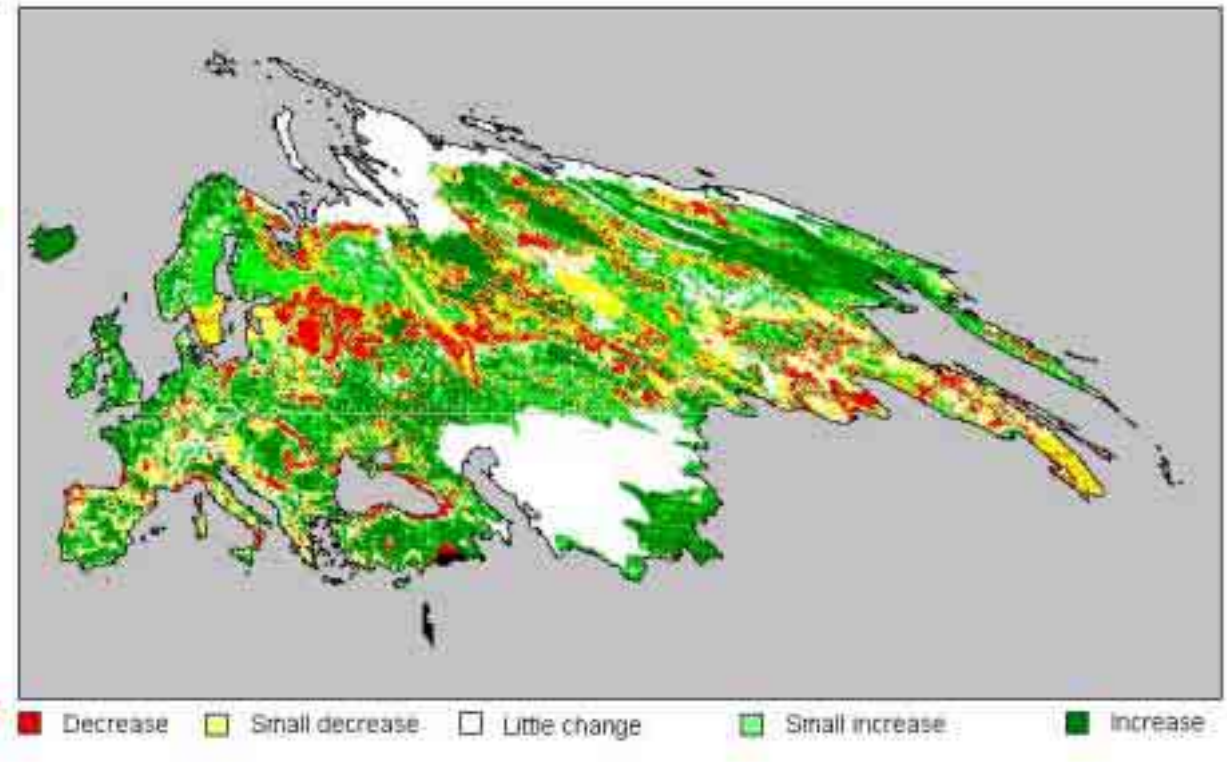

Figure 4: Simulated changes in forest cover between time 0 and 10 using simulated 1-m Ikonos data

Sample designs

FRA 2000 used a stratified random sample of Landsat scenes for the global tropics. Pre-stratification was based on ecological zones and continents (FAO 1996). Within each stratum, further stratification was introduced to reduce variance. These sub-strata are based on the prevalence of forest cover (10-40%, 40-70%, and 70-100%), which was estimated for every sub-national unit (e.g., state, municipality) in the tropics. The Landsat World Reference System (Landsat path/rows) were superimposed on the sub-national unit boundaries, and each Landsat scene was assigned to a substratum. Sample size in each stratum was proportional to the expected rate of deforestation, which was estimated for each sub-national unit based on the prevalence of forest, human population size, and *per capita* income.

The FRA 1990 pan-tropical remote sensing survey was planned in 1992. During the past 10 years, better pre-stratification materials have become globally available through coarse-resolution satellite data (AVHRR, and soon, MODIS). Use of Landsat data, with 30-m resolution, has become less expensive and more automated. For example, the USA recently completed its first national land cover map with 1992 Landsat data from 500 scenes, and a project has begun to provide similar global coverage with Landsat[6]. Also, satellite data with 1-m resolution are also available for consideration in global applications. These developments offer new options for FRA 2010. Multi-resolution satellite data would work well with multi-

[6] http://www.earthsat.com/resources/feature_project.html

stage sampling. Double-sampling for regression with remotely sensed data could improve efficiency by correlating high-resolution, but expensive, estimates of forest cover and change with less expensive lower-resolution remotely sensed data. These complex sampling designs are not considered here, but they could be considered if recommended by the Kotka IV participants.

The current analysis is limited to single-stage pre-stratified random sampling. Strata are formed with 1-km data, such as the FRA 2000 global forest cover map, that covers the entire population.

Two types of stratification are evaluated:

1. Optimisation for forest cover from 1-km AVHRR data at one point in time; and

2. Optimisation using changes in 1-km AVHRR data (or 250-m MODIS data) over a 10-year time period.

Two different sizes of sampling units are considered:

3. 150x150-km Large Sampling Unit (LSU) that conforms to an image from Landsat or a similar satellite.

4. 10x10-km Small Sampling Unit (SSU) that conforms to an satellite image with 1-m resolution or a high-altitude (e.g., 1:40,000) aerial photograph.

Strata and sub-strata

The first level of stratification is the ten FRA 2000 Ecological Zones in Figure 2. These strata are used to assure that each Zone has a sufficient sample size for analysis. Each Zone is further divided into sub-strata to minimize variance of an estimate.

Optimal boundaries for each sub-stratum were formed using methods recommended by Cochran (1977:127-131). First, consider sub-strata optimised to estimate change in forest area over 10-years with the 150x150-km Large Sampling Units (LSUs). For each sampling unit, AVHRR data from 10-years apart are used to estimate the change in forest area (km^2). (The methods used to simulate multi-date AVHRR data in this analysis are given above). AVHRR estimates have significant bias caused by misclassification errors (Czaplewski 1992). However, estimates from AVHRR are correlated with estimates from Landsat and Ikonos. Since AVHRR estimates are available for all N sample units in the population, AVHRR data can be used to define the boundaries of sub-strata for all sample units.

Boundaries of sub-strata are determined by sorting all 1,473 LSUs in the hypothetical population by the AVHRR estimate of change in forest area (km^2). Then the cumulative of the square root of the AVHRR estimate is formed and divided into L equal intervals (see y axis in Figure 5, in which k=5). The AVHRR values corresponding to those intervals define the sub-strata boundaries. An equal number of samples (n_{kh}) is assigned to each sub-stratum h. Different numbers of sub-strata were investigated for $2 \leq L \leq 6$ (Cochran 1977 pp 132-134). The efficiency for L=5 was almost identical to L=6 (except for n<75); and L=5 is used for all

evaluations in this analysis. Figure 5 illustrates use of the same method for the 284,760 10x10-km SSUs in the hypothetical population. Finally, the same procedure was independently applied to AVHRR data from one point in time to optimise estimates of forest area at that time, although these are not illustrated in Figure 5.

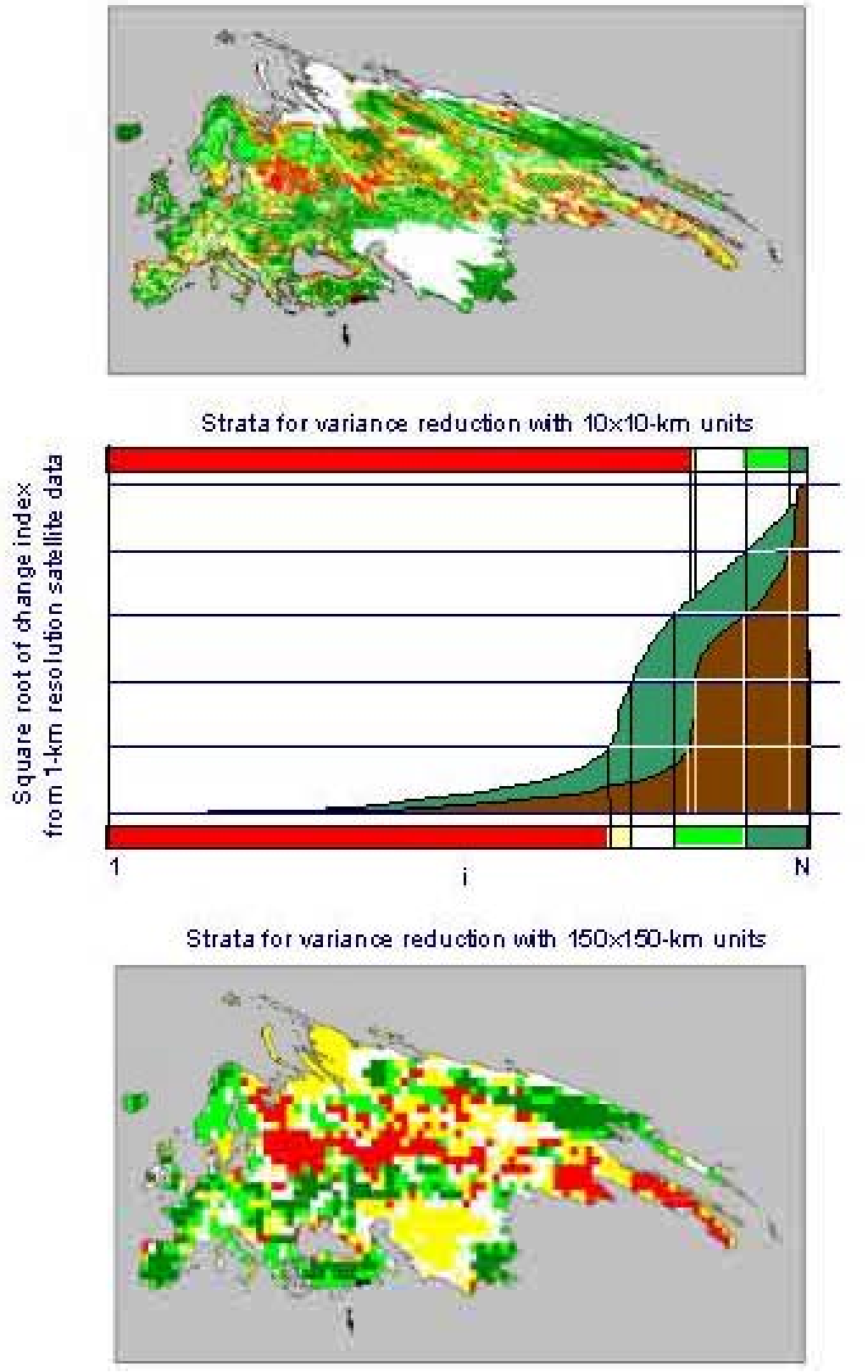

Figure 5: Stratification based on Neyman allocation for 150x150-km and 10-10-km Sample Units

Estimators

One of the unique luxuries with this type of hypothetical population is that all relevant statistics are known from the database. Therefore, the performance of alternatives statistical designs and simulated sample sizes can be determined exactly with the true totals (Y_k) and variances (S_k^2) for each ecological zone *k*. With a real population, those statistics are unknown, and they must be estimated from a single sample (i.e., y_k and s_k^2).

Using notation from Cochran (1977), the estimate for stratum *k* (ecological zone) is the sum of sub-strata (*h*) estimates:

$$Y_k = \frac{\sum_{h=1}^{L} N_{kh} Y_{kh}}{N_k}$$

$$V(Y_k) = \sum_{h=1}^{L} \left(1 - \frac{n_{kh}}{N_{kh}}\right) \frac{N_{kh}^2 S_{kh}^2}{n_{kh}}, \text{ where } S_{kh}^2 = \frac{\sum_{i=1}^{N_{kh}} (y_i - Y_{kh})^2}{N_{kh} - 1}$$

The estimate across all ecological zones is:

$$Y = \sum_k Y_k$$

$$V(Y) = \sum_k S_k^2$$

The estimates for the rate of change is computed with a Taylor series approximation (Cochran 1977).

Results

A primary purpose of the simulation is to predict the statistical accuracy of future sample estimates for FRA 2010. Accuracy is a function of sample size, and sample size affects costs.

Figure 6 summarizes the results for Europe and CIS. The standard error with the 150x150-km LSUs approaches zero as *n* approaches 1473 because of the finite population correction factor. As expected, the sub-strata boundaries optimized for forest area (using AVHRR estimates at time 0) produces more precise estimates for forest area as determined with Landsat and Ikonos data. Likewise, sub-strata boundaries optimized for changes in forest area (using AVHRR estimates at time 0 and time 10) produces more precise estimates for changes in forest area as determined with Landsat and Ikonos data.

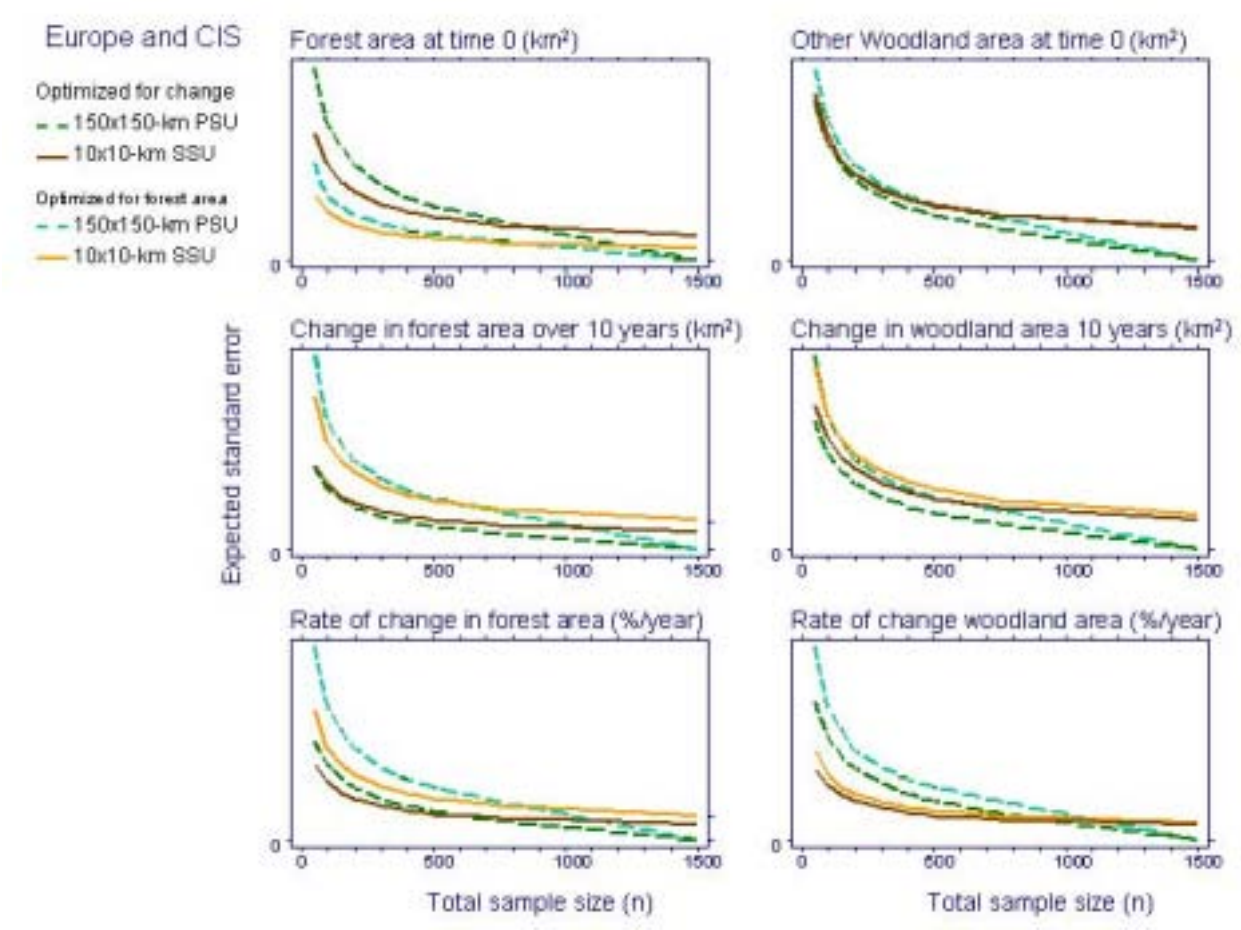

Figure 6: Standard errors expected for Europe and CIS combined

The rate of change in forest area (expressed as a proportion of forest area), is the ratio of two estimates: forest area (km^2) at time 0, and change in forest area (km^2) between times 0 and 10. Empirical results show that sub-strata optimized for change in forest area also are most efficient for estimates of rates of change (Figure 6).

Estimates for woodland are also relevant to FRA 2010. However, the sub-strata analyzed here ignore woodland statistics during optimization. Empirical results in Figure 6 show little difference among stratification alternatives in estimating woodland area at time 0. However, the stratification optimized for change in forest area is also more efficient for estimating changes in woodland area because of the positive correlation among between forest and woodland changes. This correlation is imposed by the change model used to build the hypothetical population (Table 18), and the value of these simulation results to FRA 2010 depends directly on the realism of the hypothetical population.

One surprising result is the greater efficiency with the 10x10-km sampling units (solid lines in Figure 6) relative to the 150x150-km sampling units (dashed lines in Figure 6). Larger sampling units typically have less among-unit variance than smaller sampling units, and this pattern is true with the hypothetical population. Therefore, the larger sample units usually have higher statistical efficiency when costs are not considered. This expectation does not hold true in Figure 6. The analysis was thoroughly checked for errors, and none were found. The explanation for these counter-intuitive results appears to be the methods used to optimize

sub-strata for variance reduction (Figure 5). The small sampling units can be grouped into more homogeneous sub-strata compared to the large sampling units.

Figure 7 presents similar results for one of the ten ecological zones: Boreal Coniferous Forest. This Zone has the highest rate of change among all ecological zones in the hypothetical population. The sample size *n* in Figure 7 represents the entire sample size for Europe and CIS, and only a portion of these *n* samples is allocated to the Boreal Coniferous Forest zone.

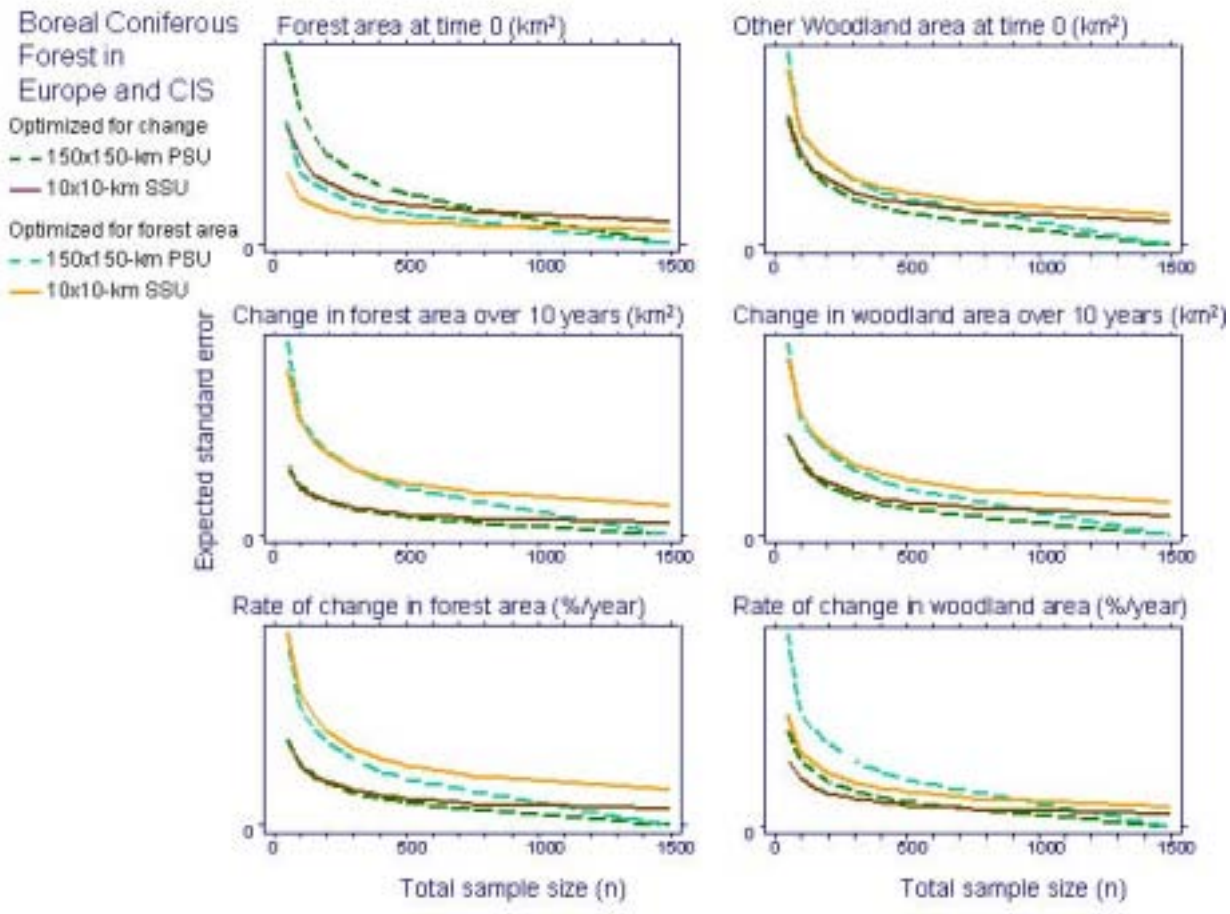

Figure 7: Standard errors expected for the Boreal Coniferous Ecological Zone

Results for the large 150x150-km sampling units in Figure 6 and Figure 7 assume that each is measured with Landsat data, not the more accurate 1-m Ikonos data. However, there is a bias in the estimates from these large sampling units caused by misclassification. Figure 8 compares the magnitude of this bias relative to the standard error. For analyses of the entire Europe and CIS region, the bias in estimated forest area at time 0 is significant except for very small sample sizes ($n<75$). The significance of this bias is somewhat less when analyzing a single ecological zone, but becomes significant in this example with a total sample size of $n\geq 300$. The bias is insignificant for estimates of changes between time 0 and time 10 for Europe and CIS, largely because the net change at this scale is only 0.16%. The bias is very notable for the Boreal Coniferous Forest zone, which has the largest loss of forest (-5.34%) among all ecological zones in this hypothetical population. The conclusion is that bias caused by misclassifications with Landsat data, relative to 1-m Ikonos data, can be large enough to be a concern for FRA 2010.

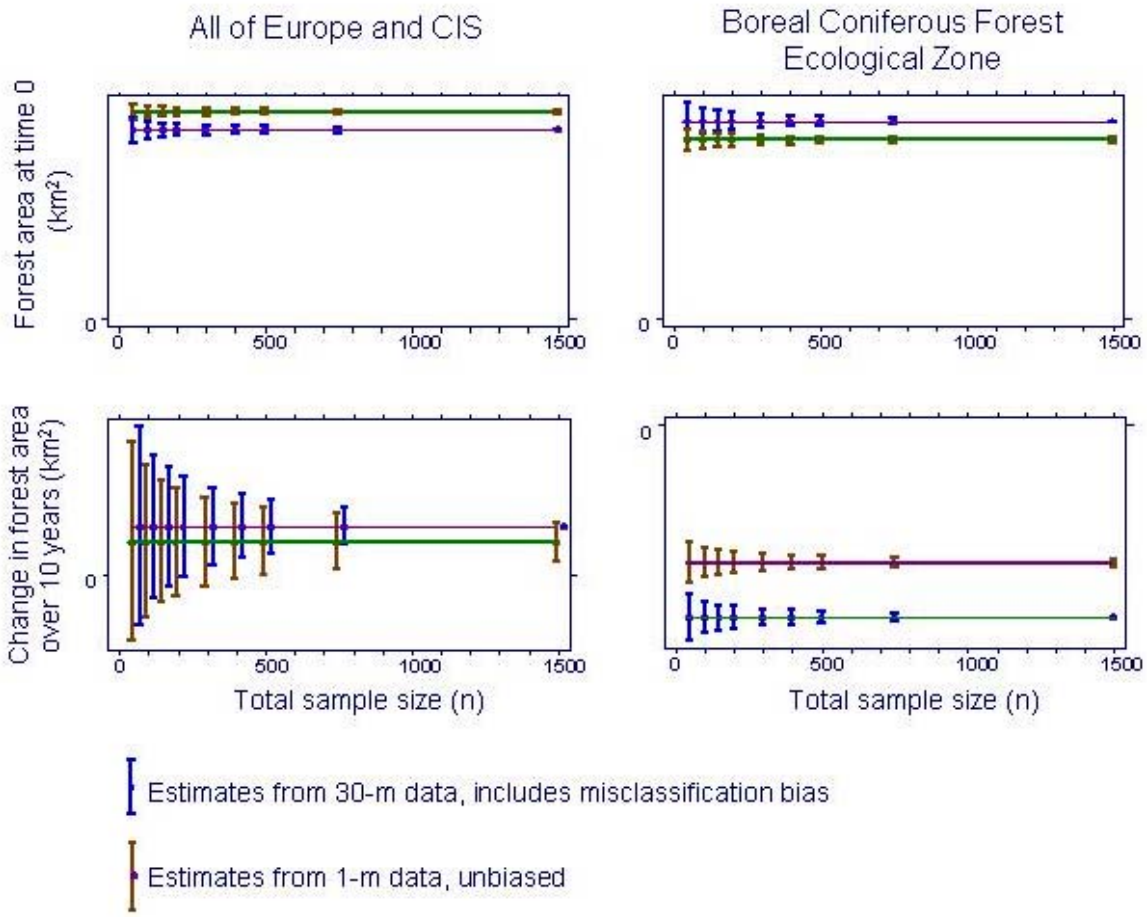

Figure 8: Expected standard errors relative to bias in Landsat estimates

Discussion

These simulations serve as a preliminary "proof-of-concept" showing one technique available to help plan for FRA 2010. Different statistical designs and degrees of complexity are possible. Results from the Kotka IV meeting will help direct these future analyses if the recommendation is to expand the remote sensing survey beyond that used for the tropics by FRA 1990 and FRA 2000.

The sample of 10x10-km Ikonos images performed unexpectedly well. However, this option would be very difficult to implement in practise. The assumption is that change detection uses two dates of imagery for the same sample unit, separated by approximately 10 years, and sub-strata are formed based on change detection with AVHRR or MODIS at the end of this time period. This will allow efficient selection of Ikonos scenes at time 10, but it is very unlikely that an Ikonos image for the same scene at time 0 is available in any archive.

It is very possible that Landsat could produce full global coverage of land cover classification in the near future. Future simulations could consider this asset. However, this product might exist for only one point in time, and sampling for change detection could remain relevant. Regardless, the FRA 2010 might assume that Landsat classifications for continental and even

global coverages will be produced by other institutions. Perhaps a unique niche for FRA 2010 among these international programs could be collection of high-resolution data from Ikonos imagery or field samples.

The value of this simulation depends directly upon the realism of the assumptions used to construct the population. If this type of work continues, then improvements should be considered. For example, the calibration models are the same for all Ecological Zones, but they would be more realistic if they were modified for each Zone. Also, the change model uses many *ad hoc* assumptions that could be improved.

Literature cited

Cochran, W.G. 1977. *Sampling techniques*. Third Edition. John Wiley & Sons, New York. 428pp.

Czaplewski, R.L. 1992. *Misclassification bias in areal estimates*. Photogrammetric Engineering and Remote Sensing. 58(2):189-192.

FAO. 1996. *Forest resources assessment 1990: Survey of tropical forest cover and study of change processes*. FAO Forestry Paper No. 130. Rome. 152pp.

FAO. 2001. *Global forest resources assessment 2000*. Main Report. FAO Forestry Paper No. 140. Rome. 479pp.

Zhu, Z. & Walter, E. 2001. *Global forest cover mapping*. FAO. FRA Working Paper No. 50 Rome. 29pp.

FAO. 2000. *Forest resources of Europe, CIS, North America, Japan and New Zealand*. Geneva Timber and Forest Study Papers No. 17. Geneva, 445pp.

Loveland, T.R., Zhu, Z., *et al.* 1999. *An analysis of the IGBP Global Land-Cover Characterization Process.* Photogrammetric Engineering and Remote Sensing, 65(9):1021-1032.

Moody, A. & Woodcock, C.E.. 1994. *Scale-dependent errors in the estimation of land-cover proportions: implications for global land-cover datasets*. Photogrammetric Engineering and Remote Sensing, 60(5):585-594.

Scepan, J. 1999. *Thematic validation of high-resolution global land-cover data sets*. Photogrammetric Engineering and Remote Sensing, 65(9):1051-1060.

Appendix 2: Additional Data on Remote Sensing Instruments

by

Kai Mäkisara

1. Introduction

This Appendix contains a review of the available remote sensing instruments supporting the discussion in Chapter 3 of this report.

2. Instruments by Class

2.1 Introduction

Based on the factors discussed in the previous section, the existing and future remote sensing instruments can be divided into several categories. The categories most useful for forest analysis are discussed below. The information presented is from numerous sources. One or two WWW addresses has been mentioned as reference where applicable. The WWW pages at these addresses contain further references.

2.2 Low-Resolution and Medium-Resolution Satellite Images (e.g., MODIS, MERIS, WIFS, AVHRR)

2.2.1 AVHRR

The best known low-resolution optical imager is probably AVHRR carried on-board the NOAA weather satellites. Depending on the model, AVHRR collects data from four or five spectral channels (see Table 24). URL http://www.ngdc.noaa.gov/seg/globsys/avhrr7.shtml

Table 24 The AVHRR spectral channels (µm).

Band number	Satellites: NOAA-6,8,10	Satellites: NOAA-7,9,11,12,14,15	Satellites: NOAA-KLM, METOP
1	0.58 - 0.68	0.58 - 0.68	0.58 - 0.68
2	0.725 - 1.10	0.725 - 1.10	0.725 - 1.0
3	3.55 - 3.93	3.55 - 3.93	1.58 - 1.64 (day) 3.55 - 3.93 (night)
4	10.50 - 11.50	10.3 - 11.3	10.3 - 11.3
5	band 4 repeated	11.5 - 12.5	11.5 - 12.5

AVHRR is a whiskbroom scanner. The pixel size at nadir is 1.1 km and the swath width 2399 km. Because of the scanning geometry, the pixel size increases with increasing scanning angle The quantisation of the pixel data is 10 bits.

AVHRR data is widely available because it can be received from the satellite using a fairly inexpensive system. Besides meteorological purposes, AVHRR data has been used in land and water applications. The continuity of AVHRR data is very good. Satellites with AVHRR have been orbiting from 1978 and the next generation of polar-orbiting weather satellites (NOAA satellites and METOP satellites) will be carrying a new version of AVHRR.

2.2.2 MODIS

The US MODIS instrument was launched on-board the Terra satellite in 1999. This satellite is a research satellite. MODIS is a very versatile instrument collecting data in 36 spectral bands (seeTable 25). The ground pixel size at nadir varies from 250 meters to 1 km depending on the channel. The swath width is 2230 km. The instrument is a whiskbroom scanner and the pixel size increases off-nadir (factor 2 along track, 5 across track). The quantisation of the data is 12 bits.URL http://modis.gsfc.nasa.gov/

Table 25 The MODIS spectral channels

band	wavelength	band	wavelength	pixel
1	620 - 670	2	841 - 876	250 m
3	450 - 470	4	545 - 565	500 m
5	1230 - 1250	6	1628 - 1652	
7	2105 - 2155			
8	405 - 420	9	438 - 448	1000 m
10	483 - 493	11	526 - 536	
12	546 - 556	13	662 - 672	
14	673 - 683	15	743 - 753	
16	862 - 877	17	890 - 920	
18	931 - 941	19	915 - 965	
20	3660 - 3840	21	3929 - 3989	
22	3929 - 3989	23	4020 - 4080	
24	4433 - 4498	25	4482 - 4549	
26	1360 - 1390	27	6535 - 6895	
28	7175 - 7475	29	8400 - 8700	
30	9580 - 9880	31	10780 - 11280	
32	11770 - 12270	33	13185 - 13485	
34	13485 - 13785	35	13735 - 14085	
36	14085 - 14385			

The most interesting channels for forest applications are 1 - 7. MODIS includes channels that can be used to estimate the characteristics of the atmosphere. These allow direct atmospheric correction of the MODIS data. The MODIS ground segment defines 44 different data products ranging from radiance counts to atmospherically corrected radiance to products like the leaf area index (LAI) and even land cover type (17 IGBP classes).

The MODIS design life is six years. Another MODIS instrument has been launched on the Aqua spacecraft in May 2002. The future of the MODIS instruments beyond this is not defined yet. Continuation for the MODIS type of instruments is planned in the NPP mission in 2005.

The MODIS data costs only the delivery costs if acquired from USGS or NASA. Other receiving entities may charge a price covering the costs.

2.2.3 MERIS

One of the instruments on-board the ESA Envisat research satellite is the MERIS imaging spectrometer. Envisat was launched in 2002. In principle, MERIS has 520 1.25 nm wide channels between 390 and 1040 nm. All of this data can't be downlinked to earth. The instrument is programmable and the set of channels to be downlinked can be selected. It has been decided that in normal operation MERIS will use the channel selection shown in Table 26. Other configurations may be used experimentally for short times. URL http://envisat.esa.int/instruments/meris/

Table 26 The 15 MERIS standard spectral channels.

Channel	Band centre nm	Bandwidth Nm	Potential applications
1	412.5	10	Yellow substance and detrital pigments
2	442.5	10	Chlorophyll absorption maximum
3	490	10	Chlorophyll and other pigments
4	510	10	Suspended sediment, red tides
5	560	10	Chlorophyll absorption minimum
6	620	10	Suspended sediment
7	665	10	Chlorophyll absorption and fluo. reference
8	681.25	7.5	Chlorophyll fluorescence peak
9	708.75	10	Fluo. Reference, atmospheric corrections
10	753.75	7.5	Vegetation, cloud
11	760.625	3.75	Oxygen absorption R-branch
12	778.75	15	Atmosphere corrections
13	865	20	Vegetation, water vapour reference
14	885	10	Atmosphere corrections
15	900	10	Water vapour, land

MERIS is a pushbroom scanner with pixel size 300 m (full resolution mode) or 1200 m (reduced resolution mode). (The pixel size in a pushbroom scanner is the same across the field of view if the curvature of the earth is ignored.) The swath width is 1150 km.

The ERS/Envisat data policy divides the users into two categories. Category 1 includes research and long term monitoring programmes. For this category, the data price will be set at or near reproduction cost. Other users belong to Category 2 where pricing is set by the distributors but ESA reserves the right to set a maximum price.

2.2.4 WIFS

The WIFS image on-board Indian IRS-1C/D collects data from two spectral channels (see Table 30) with 188 m pixel size. The imager consists of two cameras for each wavelength. The cameras are tilted 26 degrees. The swath width is 728 - 818 km. The cameras use linear detectors and this is why the pixel size changes more slowly than in a whiskbroom scanner. Quantisation is 7 bits. URL http://www.euromap.de/

The WIFS data is sold commercially. The price is about USD 900 for each image (774 by 774 km).

2.2.5 MOS-1/1b

The Japanese MOS-1 satellite was launched in 1987 and the MOS-1b satellite in 1990. Operation of MOS-1 finished in 1995 and operation of MOS-1b finished in 1996. Both satellites carried a VTIR imager. It collected data on four spectral channels (0.5-0.7 µm, 6.0-7.0 µm, 10.5-11.5 µm, 11.5-12.5 µm). The pixel size at nadir was 900 m in the visible channel and 2700 m in the infrared channels. The swath width was 1500 m. URL http://www.nasda.go.jp/sat/mos1/index_e.html

2.2.6 The Spot Vegetation Instrument

In addition to the high-resolution imagers, the Spot-4 satellite (see Section 2.3.2) is carrying a low-resolution imager, the Vegetation Instrument. Spot-5 is carrying a similar instrument, named Vegetation 2. The Vegetation Programme is developed jointly by France, the European Commission, Belgium, Italy and Sweden. The instruments collect data in four spectral channels (0.43-0.47, 0.61-0.68, 0.78-0.89, and 1.58-1.75 µm). The pixel size of these whiskbroom scanners is 1 km and swath width 2250 km.

The Vegetation data is available either as a zone extracted from a single data strip or a zone extracted from a synthesis of data strips from one day or from a 10 day period. The pricing is according to the area. A typical price for a 4 million km^2 of data is between USD 150 and USD 350.

2.2.7 Future low- and medium-resolution instruments

ADEOS-II is planned to be launched in 2002. It carries the GLI imager with 36 spectral channels. The pixel size is 1 km at nadir (250 m on six channels corresponding to the Landsat TM channels) and swath width is 1600 km. Quantisation is 12 bits. URL http://www.nasda.go.jp/sat/adeos2/index_e.html

2.3 High-Resolution Optical Satellite Image Data (e.g., Landsat TM, ETM+, Spot, IRS-1)

The high-resolution optical sensors have pixel size in the range of tens of meters. The light from the sun reflected by the targets is collected using several wavelength channels. Some sensors include also one or more channels sensing the thermal radiation emitted by the targets. In addition to these limited wavelength channels, some satellites have one panchromatic (wide channel in the visible/near infrared region) channel, which may have smaller pixel size than the narrower channels.

2.3.1 Landsat

The best known remote sensing satellites may be the Landsat satellites from the USA. The currently operating Landsat satellites have the numbers 5 and 7. Landsat 5 was launched in 1984 and it is still operating. Landsat 7 was launched in 1999 and it is currently collecting most of the Landsat images. A list of all the Landsat satellites up to now is in Table 27. The early Landsat satellites carried a multispectral scanner called MSS (Multi-Spectral Scanner). Landsat 4 introduced an improved sensor, called Thematic Mapper and is best known by the acronym *TM*. This is the main instrument on-board Landsat 5. Landsat 7 carries an improved version of this instrument, called Enhanced Thematic Mapper, ETM+. Both of these sensors collect data from seven spectral channels. In addition to the multispectral channels, ETM+ collects data also from one panchromatic channel with nominal pixel size of 15 meters. The wavelength ranges of the sensor channels are summarised in Table 28. URL http://landsat7.usgs.gov/, http://landsat.gsfc.nasa.gov/

Table 27 The Landsat missions.

Satellite	Launch Date	Sensors	Status
Landsat 1	7-23-72	MSS	Expired 1-6-78
Landsat 2	1-22-75	MSS	Expired 2-5-82
Landsat 3	3-5-78	MSS	Expired 3-31-83
Landsat 4	7-16-82	MSS, TM	Sensors no longer operational since 7-87;
Landsat 5	3-1-84	MSS, TM	Operational
Landsat 6	10-5-93	MSS, ETM	Lost at launch
Landsat 7	4-15-99	ETM+	Operational

Table 28 The Landsat MSS, TM, and ETM+ instrument chracteristics.

MSS		TM		ETM+	
Micrometers	**Resolution**	**Micrometers**	**Resolution**	**Micrometers**	**Resolution**
0.5 - 0.6	80 m	0.45 - 0.53	30 m	0.450 - 0.515	30 m
0.6 - 0.7	80 m	0.52 - 0.60	30 m	0.525 - 0.605	30 m
0.7 - 0.8	80 m	0.63 - 0.69	30 m	0.630 - 0.690	30 m
0.8 - 1.1	80 m	0.76 - 0.90	30 m	0.750 - 0.900	30 m
10.41 - 12.6	237 m	1.55 - 1.75	30 m	1.55 - 1.75	30 m
		10.40 - 12.50	120 m	10.40 - 12.50	60 m
		2.08 - 2.35	30 m	2.09 - 2.35	30 m
				0.52 - 0.90	15 m

The pixel data is digitised using eight bits. This limits the dynamic range and may be a problem in visible wavelength channels with forest targets.

The nominal width on ground of the Landsat images is about 185 km. The orbit of the Landsat satellites permit imaging of the same size every 16 days. The orbits of Landsat 5 and Landsat 7 are interleaved so that the same location can be imaged every 8 days while Landsat 5 operation continues. Note that the availability of useful images is limited by the clouds.

The Landsat data has several advantages. The data has been collected using nearly similar sensors for a long time. The price of the images is currently between USD 500 and USD 2000, depending on the location and receiving station.

New satellites in the Landsat series are in early phase of design. The sensors will have channels matching the TM and ETM channels to maintain data continuity. In addition to this, some new channels may be added. The next Landsat launch has been planned for year 2006. (URL http: //ldcm.usgs.gov). An experimental Landsat-like sensor ALI is currently orbiting on the EO-1 satellite. URL http: //eo1.gsfc.nasa.gov/

2.3.2 Spot

The French SPOT satellites have slightly different characteristics than the Landsat satellites. The pixel sizes in the HRV sensors on the satellites are smaller than in the TM/ETM sensors but the number of spectral channels is smaller and the image size is smaller. Table 29 shows the basic characteristics of the HRV instruments on-board Spot 1 – 4. URL http://www.spotimage.fr/

Table 29 The Spot sensor characteristics.

	Multispectral	**Panchromatic**
Spectral bands (nm)	500 - 590	
	610 - 680	
	790 - 890	510 - 730

	1580 - 1750 (Spot 4)	610 - 680 (Spot 4)
Pixel size	20 x 20 m	10 x 10 m
Nbr pixels per line	3000	6000

The width of the Spot images is 60 - 80 km. The orbit of the satellite passes over the same location every 26 days. The sensor is pointable (+/- 27 degrees) and this allows imaging of the same target each 2.4 days. The pointable sensor allows also stereo imaging.

The currently orbiting satellites in the Spot series are 2, 3, 4 and 5. The latest, Spot-5 was launched in May 2002. The sensor on this satellite has pixel size of 10 m in the visible and near-infrared channels and 5 or 2.5 m in the panchromatic channel. The numbers of pixels are increased so that the image width of about 60 km is maintained. The satellite can acquire two images simultaneously using along-track pointing.

The cost of the Spot images is considerably higher than the cost of the Landsat images. A typical price for a 60 by 60 km scene is between USD 2800 - 5500 (archived images may be available for lower price).

2.3.3 IRS

India has launched up to now five IRS-1 remote sensing satellites (1A in 1988, 1B in 1991, 1E in 1993, 1C in 1995, and 1D in 1997). The satellites 1b, 1C and 1D are currently producing data (IRS-1B data not available worldwide). The instruments on board IRS-1C/D include the multispectral scanner LISS-III and the panchromatic imager PAN. The characteristics of the instruments are summarised in Table 30. URL http: //www.euromap.de/

The 7-bit quantisation in the multispectral data limits the radiometric resolution of the images

Table 30 The IRS-1C/D instrument characteristics.

	PAN	**LISS-III**	**WIFS**
Spectral channels	500 - 750 nm 5.8 m	520-590 nm 23 m	
		620-680 nm 23 m	620-680 nm 188 m
		770-860 nm 23 m	770-860 nm 188 m
		1550-1700 nm 70 m	
Swath width	70 km	142 km	810 km
Quantisation	6 bit	7 bit	7 bit

The next satellite in the series carrying multispectral instruments will be IRS-P6 (Resourcesat-1). Its launch is planned for year 2002 or 2003. It is carrying improved versions of the PAN and LISS instruments. The characteristics of these new instruments are shown in Table 31. The satellite carries also a LISS-III scanner in addition to these new instruments.

Table 31 The IRS-P6 instrument characteristics.

	LISS- IV	**AWIFS**

	PAN	MSS	
Spectral channels	500 - 750 nm 5.8 m	520-590 nm 5.8 m	520-590 nm 60-70m
		620-680 nm 5.8 m	620-680 nm 60-70 m
		770-860 nm 5.8 m	770-860 nm 60-70 m
			1550-1700 nm 60-70 m
Swath width	70 km	23.9 km	700 km
Quantisation	7 bit	7 bit	10 bit

The price of one IRS-1C/D LISS-III or PAN image is about USD 2500.

2.3.4 Other High-Resolution Optical Satellites

There are several other past, present, or future satellites carrying high-resolution optical instruments. The data from these satellites can be used to complement/supplement data from the satellites mentioned above. These satellites are either experimental, or belong to short series of satellites. The availability of images from these satellites is limited, especially on a long-term basis, and this is why these satellites are not very useful for global forest monitoring.

The Russian Resurs series currently includes two satellites with high-resolution imagers, Resurs O1-3 and Resurs O1-4. The satellites were launched in 1994 and 1998. Both carry a three-channel (0.5 - 0.67 µm, 0.65 - 0.8 µm, and 0.8 - 1.0 µm) pushbroom scanner with 29 - 45 meter pixel size across track. The swath widths are 45 km and 58 km, respectively (the scanners are similar except for the number of elements). The orbit heights are different. URL http://www.scanex.ru/stations/resurs.htm

The first Japanese earth observation satellites were MOS-1 and MOS-1b. The satellites were launched in 1987 and 1990 and operated until 1995 and 1996, respectively. One of the instruments on-board these satellites was MESSR. It consisted of four modules, two for dual channel (0.51 - 0.59 µm and 0.61 - 0.69 µm) visible range monitoring and two for dual channel (0.72 - 0.80 µm and 0.80 - 1.0 µm) near-infrared region. The pixel size was 50 meters and maximum swath width 185 km. URL http://www.nasda.go.jp/sat/mos1/index_e.html

The Japanese JERS-1 satellite carried the optical OPS sensor from 1992 to 1998. It included three visible channels, four shortwave infrared bands, and one band for stereoscopic viewing. The pixels size was 18 meters and swath width 75 meters. URL http://www.nasda.go.jp/sat/jers1/index_e.html

The Japanese ADEOS satellite carried the AVNIR high-resolution imager. Unfortunately the satellite operated only 10 months. URL http://www.nasda.go.jp/sat/adeos/index_e.html

The launch of the Japanese ALOS satellite is planned for 2004. One of the ALOS instruments is AVNIR-2. It is a multispectral imager with four channels (0.42 - 0.50 µm, 0.52 - 0.60 µm, 0.61 - 0.69 µm, 0.76 - 0.89 µm). The pixel size at nadir will be 10 meters and the swath width will be 70 km. The imager can be pointed up to 44 degrees off nadir. URL http://www.nasda.go.jp/sat/alos/index_e.html

2.4 Very High Resolution Satellite Image Data (e.g., Ikonos-1, QuickBird)

The very-high resolution instruments have pixel size around one meter. This resolution has been introduced to the non-military users only a few years ago. Most of these satellites have been designed to complement and/or to replace aerial photography in many applications. The satellites operate usually on a commercial basis. All of the satellites include a panchromatic band with high spatial resolution. Many satellites also include multispectral capacity with slightly larger pixel size than is used in the panchromatic channel.

A typical swath width of the high-resolution satellites is about 10 kilometres. This is limited basically by the downlink capacity. The satellites include pointing capability and this enables obtaining imagery from every location on earth within a reasonable time. The area covered by the satellites is constrained by the small image size.

The pricing of the very-high resolution data can be expected to change according to supply and demand.

The characteristics of the currently orbiting and some planned high-resolution satellites are summarised below.

2.4.1 Ikonos-2

Ikonos-2 (Space Imaging) was the first operational high-resolution satellite with pixel size in the one meter region. It was launched in 1999. The imager on board the satellite can collect data with one panchromatic channel (450-900 nm) and four multispectral channels (445-516 nm, 506-595 nm, 632-698 nm, 757-853 nm). The pixel size on the panchromatic channel is 1 meter and on the multispectral channels 4 meters. The swath width is 13 km and the sensor is pointable both on-track and across-track. The quantisation is 11 bits. URL http://www.spaceimaging.com/

The Ikonos-2 data is currently priced per square kilometre. The minimum order is 100 km^2. The price varies between USD 7 and USD 235 per square km depending on the geometric processing, location, included channels, and acquisition type (archive, on-demand).

2.4.2 QuickBird

The second operational one-meter satellite is QuickBird 2 (DigitalGlobe). It was launched in 2001. The imager on board this satellite can also collect data with one panchromatic channel (450-900 nm) and four multispectral channels (450-520 nm, 520-600 nm, 630-690 nm, 760-900 nm). The pixel size on the panchromatic channel at nadir is 61 cm and on the multispectral channels 2.44 meters. The nominal swath width is 16.5 km (nadir pointing). Also this instrument is pointable both along-track and across-track direction. The quantisation of the data is 11 bits. URL http://www.digitalglobe.com/

The QuickBird imagery is currently sold as single frames (no geometric correction) or data covering a defined area. The basic price of a single image is USD 6000-8000 and the price of imagery with standard geometric processing is USD 22.5-30 per square km. Additional costs are incurred for different licensing and acquisition options.

2.4.3 Eros-A1

The first satellite (A1) in the EROS series (ImageSat International) was launched in year 2000. The series is planned to consist of six satellites. The remaining five satellites will be of the B series that have slightly different specifications. Launch of EROS-B1 is planned for year 2003 and the constellation will be completed in 2005. URL
http://www.imagesatintl.com/

The EROS-A1 contains a panchromatic imager (0.5-0.9 μm) that can collect data using either 1.8 meter ("normal") or 1.0 meter ("over-sampled") pixel size. The swath width is 12.5 km and quantisation 11 bits.

The B series satellites will carry an improved panchromatic imager with pixel size 0.82 meters and swath width 16 km. The quantisation is 10 bits. These satellites can also provide multispectral imagery with four spectral channels (480-520 nm, 540-580 nm, 640-680 nm, 820-900nm). Pixel size in the multispectral images is 3.28 m.

The satellites are pointable both in the along-track and the across-track direction up to 45 degrees. The visibility of receiving stations limits the availability of images worldwide.

The current price of one EROS-A1 scene is USD 1500-2500, depending on the geometric processing. Stereo pairs without geometric correction are sold for USD 3000.

2.4.4 SPOT-5

The SPOT-5 satellite is able to produce 2.5 meter effective pixel side with the so called Supermode. It uses two overlapping sensor arrays with 5 meter pixel size. The resulting image is computed from these two images. The swath width is 60 km. URL
http://www.spotimage.fr/

2.4.5 Future systems

The high-resolution satellites have been made using low-cost technology and procedures. This may be the reason why several launch attempts have failed. The demand for very-high resolution data seems to be proven. This ensures that new satellites will be launched. However, whether a certain planned satellite will become operational is not certain.

Space Imaging is planning a successor for Ikonos but no specifications have been released. The same applies to DigitalGlobe and QuickBird.

The Orbview-3 satellite will carry a panchromatic imager (450-900nm) with 1 m pixel size and a multispectral imager with 4 channels (450-520 nm, 520-600 nm, 625-695 nm, 760-900 nm) and 4 m pixel size. The swath width will be 8 km and the imagers will be pointable across-track up to 45 degrees. The pixel data quantization is 11 bits. The launch is planned for late 2002. URL http://www.orbimage.com/

The Indian IRS-P5 (Cartosat-1) to be launched in 2003 - 2004. It will be carrying two panchromatic (500 - 750 nm) cameras, one pointing 26 degrees forward and one pointing 5 degrees backwards. These enable stereo imaging from a single orbit. The pixels size will be 2.5 meters and swath width 30 km. Quantisation is 10 bits. URL http://www.euromap.de/

The Japanese ALOS satellite will include the PRISM imager. It is able to collect simultaneously three panchromatic (520 - 700 nm) images with 2.5 meter pixel size, one 24 degrees forward, one nadir, and one 24 degrees backwards. The swath width is 35 km when all three imagers are used and 70 km for nadir only viewing. URL http://www.nasda.go.jp/sat/alos/index_e.html

2.5 SAR Data

SAR is an acronym for Synthetic Aperture Radar. It is an active microwave imager. SAR uses a side-looking antenna to achieve good resolution across track with high-enough pulse power levels. The resolution along track is sacrificed but it is enhanced by computer processing afterwards.

The parameters relevant to SARs include the wavelength range (band), transmitted and received polarisation, incidence angle, and pixel size on ground. In the microwave region the wavelength ranges have traditionally been denoted by letters. The definitions of the bands can be seen in Table 32 (only some of these bands are currently used in imaging radars).

Table 32 The radar band names and frequencies.

Name	**Nominal frequency range**	**Wavelength range**	**Specific bands used in radars**
VHF	30-300 MHz	10-1 m	138-144 MHz 216-225 MHz
P (UHF)	300-1000MHz	100-30 cm	420-450 MHz 890-942 MHz
L	1-2 GHz	30-15 cm	1.215-1.4 GHz
S	2-4 GHz	15-7.5 cm	2.3-2.5 GHz 2.7-3.7 GHz
C	4-8 GHz	7.5-3.75 cm	5.25-5.925 GHz
X	8-12 GHz	3.75-2.5 cm	8.5-10.68 GHz

Ku	12-18 GHz	2.5-1.67 cm	13.4-14.0 GHz 15.7-17.7 GHz
K	18-27 GHz	1.67-1.11 cm	24.05-24.25 GHz
Ka	27-40 GHz	1.11-0.75 cm	33.4-36.0 GHz
V	40-75 GHz	0.75-0.40 cm	59-64 GHz
W	75-110 GHz	0.40-0.27 cm	76-81 GHz 92-100 GHz
millimeter	110-300 GHz	2.7-1.0 mm	

The radar is measuring the fraction of the transmitted pulse that is received at each time. The time specifies the distance between the the target reflecting the pulse and the receiving antenna. In this way the reflection (backscatter) capabilities of different targets can be measured. In addition to the target itself, the backscattered power depends on the wavelength, the geometry of the backscattering, and the polarisations (transmitted pulse, receiver). Some combinations of these auxiliary parameters are better with some targets than others. In this way different aspects of the forest can be measured using different parameters. Best results can be obtained if several parameter combinations can be used at the same time (e.g., different polarisation combinations in a polarimetric SAR).

There are a few spaceborne SARs orbiting at the moment. These operate either in the C band or in the L band and use a limited set of polarisation combinations or incident angles. The new SARs being launched in the near future widen the choice of the polarisations and imaging geometries. Unfortunately, the bands remain the same although SARs with longer wavelength would be better for forest analysis.

The SAR processing is coherent. This can be utilised in the interferometric SAR processing with two measurements from slightly different orbits. The interferometric processing allows determination of the 3-dimensional structure of the targets to some extent. A popular application is making Digital Elevation Models (DEM). The forest is a very complicated target and the elevation model of the forest can’t be determined by the interferometric processing. However, the coherence of the responses from forest can be measured and this can be used as a feature differentiating, e.g., forest types. Coherence and interferometric SAR is currently a research topics and not suitable for operational forest analysis.

The advantage of SAR against optical instruments is that the microwaves propagate through clouds. Because of this, SAR images can be obtained at any time. The drawback is that the backscattering signal from forest is very noisy and does not allow detailed analysis of forests. SAR may be useful in separating forested and non-forested areas at some locations in the world.

The SAR images are strongly influenced by the moisture of the imaged targets. This can be used as an advantage by using several images from one area from different times. In many forest application this is a necessity and increases the number of images necessary for the application.

2.5.1 ERS-1/2

The ESA ERS-1 satellite was launched in 1991 and it is still operational. The ERS-2 satellite was launched in 1995 and it is also operational. Both include a C-band SAR (wavelength 5.6 cm) that can operate in either imaging or wave mode. In imaging mode the SAR collects images with 30 m resolution and 80 km swath width. The incidence angle is 20.1 - 25.9 degrees. The polarisation is VV (vertical polarisation in both transmitter and receiver). URL http://earth.esa.int/ers/

The data policy described with MERIS applies also to ERS-1/2 data.

2.5.2 JERS-1

The Japanese JERS-1 satellite is carrying, in addition to the high-resolution optical imager, a SAR. The satellite was operational between 1992 and 1998. The SAR operated in the L-band (wavelength 23 cm). The pixel size was 18 by 18 meters and swath width 75 km. The incidence angle was 36 - 41 degrees. The polarisation is HH. URL http://www.nasda.go.jp/sat/jers1/index_e.html

JERS-1 data is available on commercial terms.

2.5.3 Radarsat

The Canadian Radarsat-1 was the first satellite in the commercial series. It was launched in 1995 and is still operational. The SAR on-board this satellite operates in the C-band (wavelength 5.6 cm) with HH polarisation. It is a very versatile imager that can operate in several different imaging modes with different pixel size, swath width and incidence angle. In standard mode, one of seven incidence angle ranges (20-27.4, 24.2-31.2, 30.4-36.9, 33.6-39.6, 36.5-42.2, 41.4-46.5, 44.9-49.4 degrees) can be chosen. The pixel size is about 25 meters and swath width about 100 km. In wide swath mode, two incidence angle ranges are available. The pixel size is about 30 m and swath width 150 km. In fine-beam mode, five incidence angle ranges between (36.9-40.1, 39.3-42.3, 41.6-44.2, 43.6-46.0, 45.3-47.8 degrees). The pixel size 9 meters and swath width 50 km. The ScanSAR modes scan over two to four wide swath beams. The resolution is 50 or 100 meters and the swath width 300-500 km. In the extended high mode the incidence angle is between 50 and 60 degrees, pixel size 25 m and swath width 50 km. In the extended low mode the incidence angle is between 10 and 20 degrees, pixel size about 25 m and swath width 75 km. URL http://www.rsi.ca/

The cost of Radarsat data for single images is about 3000 USD per image. Significant volume discounts are available.

Launch of the Radarsat-2 satellite is planned for 2003. It will have imaging modes similar to Radarsat-2. Additional ultra-fine modes with pixel size 3 by 3 m and swath width 10-20 km have been added. The third satellite, Radarsat-3 is also being planned.

2.5.4 Envisat ASAR

One of the instrument on the ESA Envisat satellite is ASAR. It is a flexible SAR operating in the C-band. In addition to the different pixel sizes and incidence angles, ASAR can also use different polarisations. ASAR can be in one of the following operating modes:

- Global monitoring mode: ScanSAR mode with 1 km pixel and 405 km swath, HH or VV polarisation.
- Wave mode: 5 x 5 km vignettes each 100 km along track, HH or VV polarisation.
- Image mode: 30 m pixel, HH or VV polarisation, other parameters in Table 35
- Alternating polarisation mode: Image mode but polarisation alternating from subframe to subframe. Results in two images (HH/VV or HH/HV or VV/VH polarisation pairs)
- Wide swath mode: ScanSAR, 405 km swath with 150 km pixel, HH or VV polarisation

URL http://envisat.esa.int/

Table 33 ASAR image mode products.

ASAR Swathes	Swath Width [km]	Near Range Incidence Angle	Far Range Incidence Angle
IS1	108.4 - 109.0	14.1 - 14.4	22.2 - 22.3
IS2	107.1 - 107.7	18.4 - 18.7	26.1 - 26.2
IS3	83.9 - 84.3	25.6 - 25.9	31.1 - 31.3
IS4	90.1 - 90.6	30.6 - 30.9	36.1 - 36.2
IS5	65.7 - 66.0	35.5 - 35.8	39.2 - 39.4
IS6	72.3 - 72.7	38.8 - 39.1	42.6 - 42.8
IS7	57.8 - 58.0	42.2 - 42.6	45.1 - 45.3

The Envisat data policy described previously with MERIS applies also to ASAR.

2.5.5 Future SAR satellites

The Japanese ALOS satellite (launch planned for 2004) will carry the PALSAR imager. It is operating in the L-band (wavelength 23 cm) and can be in one of three modes. In the high-resolution mode the pixel size is 10 m and swath width is 70 km. In high resolution mode it can collect data with 10-50 m pixel size and 40-70 km swath width. It can operate in either HH or VV polarisation mode or in combined HH+HV or VV+VH modes. The incidence angle can be selected between 8 and 60 degrees. In ScanSAR mode it can image 250-350 km swath with 100 m pixel size. The polarisation is either HH or VV and the incidence angle 8-43 degrees. Additionally this SAR has an experimental polarimetric mode with 24-89 m pixel size and 20-65 km swath width.

There are several other SAR satellites or satellite constellations under different stages of planning, including TerraSAR and Cosmo Skymed.

2.5.6 Airborne SAR

There exist several airborne SAR systems. Most of these are research systems, like the JPL AIRSAR, the German ESAR, the Danish EMISAR, and the Canadian CCRS C/X-SAR. There also exist at least commercial airborne SAR systems. One of these is Intermap Star-3i SAR (URL http://www.globalterrain.com/Technology.html). However, this is an X-band SAR and not very useful in forest applications.

2.6 Laser Scanners and LIDARs

Laser scanners and LIDARs are active instruments operating in the visible or infrared range. Narrow pulses are produced by a laser is sent towards a target and the received light energy and arrival time are measured. The time gives the distance between the instrument and the target whereas the intensity of the received light reflects the properties of the target (and the atmosphere). In many cases the instruments measure only the time of return of the pulses. In this case the instrument measures only the distance. There may be several returned pulses corresponding to one sent pulse in case the pulse energy is reflected by several targets. In forest applications this can mean reflections from the target and the ground, in which case the instrument can be used to measure the height of the trees. In addition to these reflections, there are reflections from other targets between the top of canopy and the ground.

Image data can be formed by scanning the laser and sensor over the target area while the platform is moving forward.

A laser scanner has been used in space on two Space Shuttle flights. The first mission, SLA-1 (Shuttle Laser Altimeter) was on STS-72 (74) 1996 and the second mission was SLA-2 on STS-85 in 1997. Some forest data from low latitudes was collected on these flights.

The first spaceborne LIDAR applicable to forest analysis will be the US Vegetation Canopy LIDAR (VCL). The launch of this satellite is planned for 2003. The inclination of the orbit is 67 degrees and this limits the data to latitudes below 67 degrees. The instrument uses three fixed lasers operating at 1064 nm. The ground tracks of the lasers are spaced by 4 km apart on the ground and the pulse spacing along track is nearly contiguous. The footprint of each laser is 25 m and the expected canopy top height and ground elevation accuracy is 1 m. URL http://www.geog.umd.edu/vcl/

There are a few airborne laser scanners operating in the world. These can be used to obtain accurate tree height data from limited areas. The pixel size of these instruments is about 1 m and the height accuracy is about 20 cm. Considering the inaccuracies in locating the tree tops and combining the errors, the accuracy of tree height measurements is about 0.5 m - 1m.

2.7 Imaging Spectrometer Data

An imaging spectrometer is an optical imager that can collect data simultaneously using a large number of narrow spectral channels. The spectral channels are contiguous or a subset of contiguous channels. The advantage of imaging spectrometers is that they can very accurately analyse the spectra of different targets. Whether this is useful or not, depends on the application. In forest applications the success has so far been moderate.

Most of the current imaging spectrometers are airborne instruments (e.g., AVIRIS, CASI, AISA, DAIS, ROSIS, MIVIS). The best known airborne imaging spectrometer is AVIRIS. It can collect 224 channels in the wavelength range 380-2500 nm (10 nm channels). It is flying at 20 km altitude with pixel size 20 m and 11 km swath or at 4 km altitude with pixel size 4 m and 2 km swath. URL http://makalu.jpl.nasa.gov/aviris.html

The CASI and AISA instruments are operating in the visible and infrared range (450-900 nm). Both are programmable and can be flown on small aircrafts with varying pixel size. URLs http://www.itres.com, http://www.specim.fi/

The first spaceborne, earth-viewing imaging spectrometer is Hyperion on the NASA EO-1 experimental satellite. It was launched in year 2000 and is still operating. The spectrometer can collect data with 220 spectral channels in the wavelength range 400-2500 nm. The pixel size is 30 m and swath width is 7.5 km. URL http://eo1.gsfc.nasa.gov/

The US NAVY NEMO (Naval Earth Map Observer) satellite is planned to be launched in 2002. One of its instruments is the COIS (Coastal Ocean Imaging Spectrometer) spectrometer. It collects data using 10 nm spectral channels in the wavelength range 400-2500 nm (210 bands). The pixel size is 30 or 60 m and the swath width is 30 km. The PIC (Panchromatic Imaging Camera) camera can be used to simultaneously image the same area with 5 m pixel size. NEMO will be downlinking spectral signature recognition data instead of raw data. URL http://nemo.nrl.navy.mil/

The plans for the Australian ARIES-1 (Australian Resource Information and Environment Satellite) satellite are not clear at the moment. It should be carrying an imaging spectrometer operating in the 400-2500 nm range and a panchromatic camera.

2.8 Aerial photography

The most important airborne data source is aerial photography in various forms. It is being commercially used all over the world and provides spatially accurate images over limited areas. In some countries, even countrywide aerial photograph archives exist or are being planned.

Aerial photography can be divided into classes based on the film type, flight altitude, resolution, and image format.

The film type is usually either panchromatic, colour, or false colour. In the false colour film, one of the layers is sensitive to red light, one to green light, and one to near infrared light. The pigments have been arranged so that the red light is shown as green, green light as blue, and infrared as red. The vegetation reflects infrared light and the red areas in the false-colour images correspond to vegetation.

The aerial photographs on film are usable for visual analysis but not for any automatic analysis. The photographs can be transformed into digital form by scanning. Currently there exist high-quality scanners that can be used operationally. The tendency is to move to digitised aerial photographs also for visual use because the geometric processing and archiving are easier.

There are some completely digital aerial photography cameras nowadays. However, the pressure to develop digital cameras is not high because the digitised analog photographs work well enough. The completely digital systems provide better geometric stability and they can be calibrated radiometrically (an advantage in numerical analysis of the images).

The area covered by the photographs and the smallest usable details depend on the size of the film, the optical system of the camera, and the flight altitude. Usually the aerial photographs are characterised by the scale. When the digitisation pixel size is known, this enables computation of the pixel size on ground. For instance, assuming scale 1: 30000 and pixel size 20 μm (typical values), we get the pixel size 0.6 m.

With a fixed scale, the film size, the area being digitised, and the desired overlap (30-60 %) determine the number of images needed. The typical film width of the metric cameras used in aerial photography is 240 mm (230 by 230 mm image area). With 1: 30000 scale this gives the image size 6.9 by 6.9 km on ground. Narrower film (70 mm or 35 mm) or video cameras are used in detailed photography but these formats are less suitable for covering larger areas.

The price of digital photography varies according to the imaging parameters and supplier. A typical price level for a set of high-altitude aerial photographs mosaiced to a geocoded orthophoto is about USD 0.15 per hectare. However, the price varies widely according to the scale and whether existing imagery can be used or new flights are required.

3. Covering the Whole Earth with Images

The land area of the world (excluding Antarctica) is about 135 000 000 km^2. If we assume that there is 10 % overlap between the images, the images should cover an area of 148 500 000 km^2. Rough estimates of the numbers of images needed to cover the land areas of the Earth are given in Table 34. The image height is assumed to be equal to the image width although in practice this does not always apply. The height of the images from lower resolution satellites often is limited only by the receiving station visibility. The prices are computed according to the current price lists for single images. AVHRR and MODIS data can be obtained by paying the handling costs and the total cost is not computed for these data sources.

Table 34 The number of images needed to cover the land area of the Earth for different satelliteinstruments. The amount of data per channel is computed assuming rectification to the nadir pixel size. The number of channels is the maximum number of channels usable in forest applications.

Satellite	**Nbr. images**	**Gigabytes per channel**	**Channels**	**Price**
AVHRR	26	0.25	5	N.A.
MODIS	30	0.30 - 1.2	7 (36)	N.A.
Landsat TM/ETM+	4 339	165 - 660	7 (8)	2.2 - 8.7 Million USD
Spot HRV	41 250	370 - 1 480	4/5	100 - 200 Million USD
IRS LISS-III	7 365	280	4	20 Million USD
QuickBird	545 455	25 000 - 100 000	4	3 800 Million USD

Table 34 shows that it is feasible to cover the whole earth with low-resolution data (AVHRR, MODIS) but using medium-resolution data is questionable. The amount of data is within limits of the processing capabilities of reasonable computers. The price is not reasonable but a mosaic made for research purposes by some organisation may be available for a fraction of this price. The high-resolution data is clearly usable only for local sampling.

FRA Working Papers

0. How to write a FRA Working Paper (10 pp. – E)
1. FRA 2000 Terms and Definitions (18 pp. - E/F/S/P)
2. FRA 2000 Guidelines for assessments in tropical and sub-tropical countries (43 pp. - E/F/S/P)
3. The status of the forest resources assessment in the South-Asian sub-region and the country capacity building needs. Proceedings of the GCP/RAS/162/JPN regional workshop held in Dehradun, India, 8-12 June 1998 (186 pp. - E)
4. Volume/Biomass Special Study: georeferenced forest volume data for Latin America (93 pp. - E)
5. Volume/Biomass Special Study: georeferenced forest volume data for Asia and Tropical Oceania (102 pp. - E)
6. Country Maps for the Forestry Department website (21 pp. - E)
7. Forest Resources Information System (FORIS) – Concepts and Status Report (20 pp. E)
8. Remote Sensing and Forest Monitoring in FRA 2000 and beyond (22 pp. - E)
9. Volume/Biomass special Study: Georeferenced Forest Volume Data for Tropical Africa (97 pp. – E)
10. Memorias del Taller sobre el Programa de Evaluación de los Recursos Forestales en once Países Latinoamericanos (194 pp. - S)
11. Non-wood forest Products study for Mexico, Cuba and South America (draft for comments) (82 pp. – E)
12. Annotated bibliography on Forest cover change – Nepal (59 pp. – E)
13. Annotated bibliography on Forest cover change – Guatemala (66 pp. – E)
14. Forest Resources of Bhutan - Country Report (80 pp. – E)
15. Forest Resources of Bangladesh – Country Report (93 pp. – E)
16. Forest Resources of Nepal – Country Report (78 pp. - E)
17. Forest Resources of Sri Lanka – Country Report (77 pp. – E)
18. Forest plantation resource in developing countries (75 pp. – E)
19. Global forest cover map (14 pp. – E)
20. A concept and strategy for ecological zoning for the global FRA 2000 (23 pp. – E)
21. Planning and information needs assessment for forest fires component (32 pp. – E)
22. Evaluación de los productos forestales no madereros en América Central (102 pp. – S)
23. Forest resources documentation, archiving and research for the Global FRA 2000 (77 pp. – E)
24. Maintenance of Country Texts on the FAO Forestry Department Website (25 pp. – E)
25. Field documentation of forest cover changes for the Global FRA 2000 (40 pp. – E)
26. FRA 2000 Global Ecological Zones Mapping Workshop Report Cambridge, 28-30 July 1999 (53 pp. –E)
27. Tropical Deforestation Literature:Geographical and Historical Patterns in the Availability of Information and the Analysis of Causes (17 pp. – E)
28. Global Forest Survey – Concept Paper (30 pp. - E)
29. Forest cover mapping and monitoring with NOAA-AVHRR and other coarse spatial resolution sensors (42 pp. - E)
30. Web Page Editorial Guidelines (22 pp. – E)
31. Assessing state & change in Global Forest Cover: 2000 and beyond (15 pp. – E)
32. Rationale & methodology for Global Forest Survey (60 pp. – E)
33. On definitions of forest and forest change (13 pp.- E)
34. Bibliografía comentada. Cambios en la cobertura forestal: Nicaragua (51 pp. – S)
35. Bibliografía comentada. Cambios en la cobertura forestal: México (35 pp. – S)
36. Bibliografía comentada. Cambios en la cobertura forestal: Costa Rica (55 pp. – S)
37. Bibliografía comentada. Cambios en la cobertura forestal: El Salvador (35 pp. – S)
38. Bibliografia comentada. Cambios en la cobertura forestal: Ecuador (47 pp. – S)
39. Bibliografia comentada. Cambios en la cobertura forestal: Venezuela (32 pp. – S)
40. Annotated bibliography. Forest Cover Change: Belize (36 pp. – E)
41. Bibliografia comentada. Cambios en la cobertura forestal: Panamà (32 pp. – S)
42. Proceedings of the FAO Expert consultation to review the FRA 2000 methodology for Regional and Global Forest Change Assessment (54 pp. – E)
43 Bibliografia comentada. Cambios en la cobertura forestal: Colombia (32 pp. – E)
44 Bibliografia comentada. Cambios en la cobertura forestal: Honduras (42 pp. – E)
45 Proceedings of the South-Asian Regional Workshop on Planning, Database & Networking for Sustainable Forest Management (254 pp. – E)
46 Missing
47 Proceedings of the Regional workshop on forestry information services, Stellenbosch, South Africa, 12-17 feb. 2001
48 Forest cover assessment in the Argentinean Regions of Monte and Espinal (25 pp. – E)
49 Under preparation

50 Global Forest Cover Mapping – Final Report (29 pp. – E)
51 FAO Workshop Data Collection for the Pacific Region, 4-8 September 2000, Apia, Samoa (370 pp. - E)
52 Under preparation
53 Forest occurring species of conservation concern: Review of status of information for FRA 2000 (E)
54 Assessing Forest Integrity and Naturalness in Relation to Biodiversity(64 pp.)
55 Global Forest Fire Assessment 1990-2000 (495 pp. – E)
56 Global Ecological Zoning for the Global FRA 2000 – Final Report (210 pp. – E)
57 Missing
58 Missing
59 Comparison of forest area and forest area change estimates derived from FRA 1990 and FRA 2000 (70 pp. - E)
60 On sampling for estimating global tropical deforestation (12 pp. - E)
61 The role of remote sensing in global forest assessment (73 pp. - E)

Please send a message to fra@fao.org for electronic copies or download from
www.fao.org/forestry/fo/fra/index.jsp (under Publications)